

การคัดกรองของอะลูมินาในน้ำที่ปราศจากไอออน



นางสาววิภาดา ดอกไม้

จุฬาลงกรณ์มหาวิทยาลัย

CHULALONGKORN UNIVERSITY

บทคัดย่อและแฟ้มข้อมูลฉบับเต็มของวิทยานิพนธ์ตั้งแต่ปีการศึกษา 2554 ที่ให้บริการในคลังปัญญาจุฬาฯ (CUIR)  
เป็นแฟ้มข้อมูลของนิสิตเจ้าของวิทยานิพนธ์ ที่ส่งผ่านทางบัณฑิตวิทยาลัย

The abstract and full text of theses from the academic year 2011 in Chulalongkorn University Intellectual Repository (CUIR)  
are the thesis authors' files submitted through the University Graduate School.

วิทยานิพนธ์นี้เป็นส่วนหนึ่งของการศึกษาตามหลักสูตรปริญญาวิศวกรรมศาสตรมหาบัณฑิต

สาขาวิชาวิศวกรรมเคมี ภาควิชาวิศวกรรมเคมี

คณะวิศวกรรมศาสตร์ จุฬาลงกรณ์มหาวิทยาลัย

ปีการศึกษา 2557

ลิขสิทธิ์ของจุฬาลงกรณ์มหาวิทยาลัย

ALUMINA CORROSION IN DEIONIZED WATER

Miss Vipada Dokmai



A Thesis Submitted in Partial Fulfillment of the Requirements  
for the Degree of Master of Engineering Program in Chemical Engineering

Department of Chemical Engineering

Faculty of Engineering

Chulalongkorn University

Academic Year 2014

Copyright of Chulalongkorn University

Thesis Title	ALUMINA CORROSION IN DEIONIZED WATER
By	Miss Vipada Dokmai
Field of Study	Chemical Engineering
Thesis Advisor	Associate Professor Varong Pavarajarn, Ph.D.

---

Accepted by the Faculty of Engineering, Chulalongkorn University in Partial Fulfillment of the Requirements for the Master's Degree

.....Dean of the Faculty of Engineering  
(Professor Bundhit Eua-arporn, Ph.D.)

THESIS COMMITTEE

.....Chairman  
(Associate Professor Tawatchai Charinpanitkul, D.Eng.)

.....Thesis Advisor  
(Associate Professor Varong Pavarajarn, Ph.D.)

.....Examiner  
(Associate Professor Anongnat Somwangthanaroj, Ph.D.)

.....External Examiner  
(Duangporn Sompongse, Ph.D.)

วิภาดา ดอกไม้ : การกัดกร่อนของอะลูมินาในน้ำที่ปราศจากไอออน (ALUMINA CORROSION IN DEIONIZED WATER) อ.ที่ปรึกษาวิทยานิพนธ์หลัก: รศ. วรงค์ ปวราจารย์, 91 หน้า.

พฤติกรรมการกัดกร่อนของชั้นอะลูมินาในน้ำที่ปราศจากไอออนได้ถูกศึกษา งานวิจัยนี้จะมุ่งเน้นไปที่อะลูมินาที่มีโครงสร้างแบบอสัณฐาน ซึ่งมาจากกระบวนการสปีดเตอริงที่พบได้ในอุตสาหกรรมไมโครอิเล็กทรอนิกส์โดยทั่วไป การทดสอบการกัดกร่อนกระทำโดยการนำชิ้นงานที่มีชั้นอะลูมินาดังกล่าวมาจุ่มลงในน้ำที่ปราศจากไอออนที่อุณหภูมิตั้งแต่ 25 ถึง 80 องศาเซลเซียส ในช่วงเวลาที่แตกต่างกัน ผลจากการวิเคราะห์ด้วยกล้องจุลทรรศน์แบบส่องกราดแสดงให้เห็นว่าข้อบกพร่องเริ่มก่อตัวขึ้นบนชิ้นงาน ณ อุณหภูมิ 50 องศาเซลเซียส ซึ่งจะมีระดับที่รุนแรงขึ้นเมื่ออุณหภูมิและเวลาในการสัมผัสเพิ่มมากขึ้น เมื่อนำชิ้นงานดังกล่าวมาตรวจสอบหาหมู่ฟังก์ชันที่เกิดขึ้นด้วยการวิเคราะห์ฟูเรียทรานสฟอร์มอินฟราเรดสเปกโตรสโคปี พบว่าจะสังเกตเห็นพันธะ O-H ในปริมาณที่สูงขึ้นเมื่อข้อบกพร่องก่อตัวบนชิ้นงาน ดังนั้นจึงกล่าวได้ว่าข้อบกพร่องที่เกิดขึ้นเป็นผลมาจากปฏิกิริยาไฮโดรไลซิสระหว่างอะลูมินาแบบอสัณฐานกับน้ำ นอกเหนือจากนั้นในงานนี้ยังได้ศึกษาปัจจัยอื่นที่อาจจะก่อให้เกิดการกัดกร่อนเช่น ผลของค่าความเป็นกรด-เบสในน้ำ ผลของไอออนชนิดต่างๆที่ปะปนอยู่ในสารละลาย ปริมาณออกซิเจนที่ละลายอยู่ในน้ำ ผลของการถ่ายโอนอิเล็กตรอนระหว่างพื้นผิว เป็นต้น ทั้งนี้เพื่อที่จะนำมาอธิบายปรากฏการณ์ดังกล่าวและนำมาสู่การป้องกันปัญหานี้ ตลอดจนสามารถใช้เป็นความรู้พื้นฐานในการปรับปรุงหรือพัฒนาอุตสาหกรรมไมโครอิเล็กทรอนิกส์ต่อไปในอนาคต

จุฬาลงกรณ์มหาวิทยาลัย  
CHULALONGKORN UNIVERSITY

ภาควิชา วิศวกรรมเคมี

สาขาวิชา วิศวกรรมเคมี

ปีการศึกษา 2557

ลายมือชื่อนิสิต .....

ลายมือชื่อ อ.ที่ปรึกษาหลัก .....

# # 5670380921 : MAJOR CHEMICAL ENGINEERING

KEYWORDS: AMORPHOUS ALUMINA / CORROSION / DEIONIZED WATER

VIPADA DOKMAI: ALUMINA CORROSION IN DEIONIZED WATER. ADVISOR:  
ASSOC. PROF. VARONG PAVARAJARN, Ph.D., 91 pp.

The corrosion behavior of alumina ( $\text{Al}_2\text{O}_3$ ) layer after exposed to deionized water (DI) is studied. This work focuses on the amorphous alumina which is formed via sputtering process, the process that can be found in many microelectronic industries. The corrosion test was conducted by immersing the alumina coated coupon in DI water at different temperature (from 25-80°C) and various period of time. The formation of the corrosion in terms of defect formed on the surface of the coupon is monitored by using scanning electron microscopy (SEM). From the result, it showed that the defect begins appearing at 50°C, and tends to become severe when the temperature and the immersion time were increasing. Fourier transform infrared spectroscopy (FTIR) indicated that the main functional group of O-H is found after the defect was formed on the surface. Therefore, it is pointed out that such defect is a result from hydrolysis reaction between amorphous alumina and water. The effect of other factors such as pH of water, ions in water, the amount of oxygen dissolved in water and the electron transfer are also investigated and reported. The obtained results are not only aimed to describe this phenomenon or lead to the prevention of this problem but also important as fundamental understanding about the corrosion behavior in basic solution. This knowledge can be used for further improvement and application in microelectronic industries.

Department: Chemical Engineering

Student's Signature .....

Field of Study: Chemical Engineering

Advisor's Signature .....

Academic Year: 2014

## ACKNOWLEDGEMENTS

I would like to sincere gratitude to my thesis advisor, Associate Professor Dr. Varong Pavarajarn at department of chemical engineering, Chulalongkorn University for his helpful, extensive guidance, valuable suggestion, deep discussion and encouragement to pass obstacles throughout of this work.

I would also like to thank Associate Professor Dr. Tawatchai Charinpanitkul as the chairman, Associate Professor Dr. Anongnat Somwangthanaroj and Dr. Duangporn Sompongse for their useful discussions and participation as thesis committee.

Additionally, I am particularly grateful to Western Digital Thailand Co., Ltd. for providing alumina-coated coupons, technical guidance and analytical technique as well as financial support.

Furthermore, I also extend my thanks to the Center of Excellence in Particle Technology, Department of Chemical Engineering, Chulalongkorn University for their partial support and all my friends who always provide assistance and encouragement.

Finally, I would like to especially thank and appreciate my parents who always love, support and advise throughout the course of my life.

## CONTENTS

	Page
THAI ABSTRACT .....	iv
ENGLISH ABSTRACT .....	v
ACKNOWLEDGEMENTS .....	vi
CONTENTS .....	vii
CHAPTER I INTRODUCTION .....	1
2.1 Definition and importance of corrosion .....	3
2.2 Literature reviews involve with alumina corrosion.....	4
CHAPTER III EXPERIMENTAL .....	10
3.1 Materials.....	10
3.2 Experimental Procedures.....	11
3.2.1 Replication of corrosion in laboratory.....	11
3.2.2 Experimental apparatus involved in alumina corrosion test.....	13
3.2.2.1 Apparatus for studying the effect of hydroxyl radicals in water. ..	13
3.2.2.3 Apparatus for studying the effect of oxygen content in water. ....	14
3.2.2.4 Apparatus for studying the effect of ions in water.....	16
3.2.2.5 Apparatus for studying the effect of electron transfer.....	16
3.2.2.6 Apparatus for studying the effect of the local concentration of H <sup>+</sup> /OH <sup>-</sup> .....	17
3.2.2.7 Apparatus for studying the effect of electron transfer couple with oxygen content.....	18
3.3 Characterizations .....	20
3.3.1 Scanning Electron Microscopy (SEM) .....	20
3.3.2 X-ray diffraction (XRD).....	20

	Page
3.3.3 Fourier Transform Infrared spectroscopy (FTIR).....	20
3.3.5 Point of zero charge determination.....	21
4.1 Characterizations on alumina-coated coupon.....	22
4.1.1 X-ray diffraction analysis.....	22
4.1.2 Fourier transform infrared spectroscopy analysis.....	24
4.2 Replication the corrosion of amorphous alumina in laboratory.....	25
4.3 Factors affecting the corrosion of amorphous alumina.....	32
4.3.1 The effects of OH radicals.....	32
4.3.2 The effect of water pH.....	35
4.3.3 The effect of oxygen content in water.....	39
4.3.4.1 The effect of anion.....	43
4.3.4.1 The effect of cations.....	50
4.3.5 The effect of electron transfer on the specimen.....	56
4.3.7 The effect of local $H^+/OH^-$ concentration.....	67
CHAPTER V CONCLUSION AND RECOMMENDATION.....	76
5.1 Summary of the results.....	76
5.2 Conclusions.....	77
5.3 Recommendations.....	78
REFERENCES.....	79
APPENDICES.....	83
APPENDIX A CALCULATION THE CONCENTRATION OF ION IN AQUEOUS SOLUTION ...	84
APPENDIX B MEASURING AVERAGE PARTICLE SIZE AND HIGH OF $OH^-$ PEAK.....	88
APPENDIX C CALCULATION OF AQUEOUS SOLUTION WITH ANY PH VALUES.....	90

APPENDIX D LIST OF PPUBLICATION.....	93
VITA.....	94



## CHAPTER I

### INTRODUCTION

In many industries, corrosion is a major concern because of its capability to destroy the material and leading to a lot of problems such as contamination of corrosion product, loss of product, plant shutdown, decreased mechanical efficiency and time-consuming maintenance. In some instances, the industries have to overdesign to prevent corrosion which directly affects economic costs. Moreover, there have been a few studies on the effective solution of this problem by researchers. Therefore, most of practical method applied in the industrial process is selecting suitable material with high corrosion resistance for each environmental condition [1].

Currently, alumina ceramics ( $\text{Al}_2\text{O}_3$ ) is one of the most interesting materials which plays important role in many fields [2]. Because there are good properties of this material such as high structural stability, high melting point and inert to reaction, it has higher corrosion resistance than other metals [3, 4]. The application of  $\text{Al}_2\text{O}_3$  is widely used in several works such as ceramic turbine, components of valve, nozzle, mechanical part and it is also useful for catalyst or catalyst support of reactions. Therefore, the use of  $\text{Al}_2\text{O}_3$  ceramic is popular in variety of industrials as the anti-corrosive material which depends on operating condition in each process.

In this research, the author focuses on a type of industry that has clearly been affected by the corrosion of  $\text{Al}_2\text{O}_3$  when it was exposed in deionized water,

which directly damages to the specimen. Moreover, it also resulted in the many products are rejected. In contrast with alumina's nature, it is believed that alumina is inert to chemical reaction and does not react with water under low temperature condition. Typical of industries that have obviously found a problem are hard disk drive manufacturing, and so on. Therefore, the corrosion behavior of  $\text{Al}_2\text{O}_3$  in DI water and the reaction mechanism are needed to be investigated. Also, the factors causing defects on hard disk drive products should be explained to prevent the corrosion.

For this reasons, the objectives of this project are to understand the phenomena of alumina corrosion in deionized water and to study the mechanism and factors affecting the corrosion which leads to prevention of this problem.

The research is consist of five chapters as following;

Chapter I suggests the motivation and introduction of this work.

Chapter II describes the basic theory about definition and importance of corrosion as an engineer. The literature surveys of previous reviews relating to alumina corrosion in various conditions are also mentioned in this chapter.

Chapter III presents the experimental design, material used for corrosion testing and analytical techniques.

Chapter IV shows the results and discussion of this research.

Chapter V describes the overall conclusions and recommendations of this research

## CHAPTER II

### THEORY AND LITERATURE REVIEWS

This chapter describes definition and importance of corrosion, literature reviews, which relating to alumina in various conditions and the resulting of each condition will also be explained.

#### 2.1 Definition and importance of corrosion

Corrosion is the destructive attack of material by chemical or electrochemical reaction with its environment [5]. Deterioration by physical or mechanical causes is not called corrosion, but it is described as erosion or abrasion. In general, corrosion has usually been found on metal, the cycle of corrosion as shown in Figure 2.1. On the other hand, most of nonmetals such as plastic, wood and ceramic will not be corroded because there have not free electron, but these material may swell and crack or leach away when exposed in inappropriate environmental conditions.

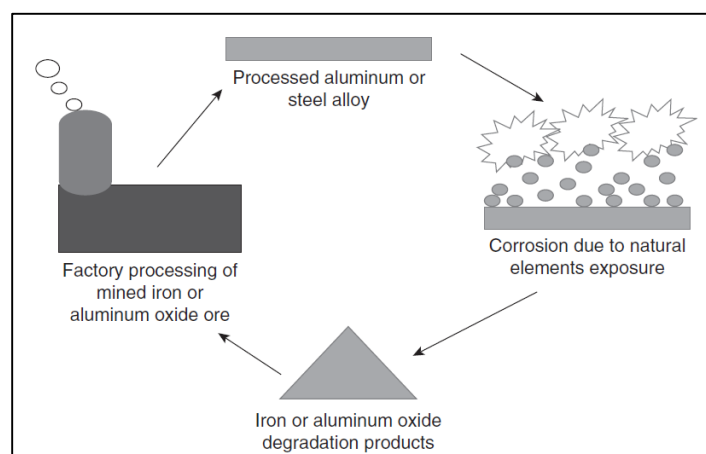


**Figure 2.1** Diagrammatic representation of corrosion cycle in general industries [5].

Corrosion processes mostly involve chemical change which is electrochemical reaction [6,7]. The corrosion is directly impacted on economic, safety and conservation which are the major concern of many industries [8]. Thus, the study on principles of chemistry is very important to understand the corrosion behavior. As for engineer, we should learn about corrosion mechanisms in order to improve the ways to prevent damage caused by corrosion and apply knowledge to control corrosion problem.

All of previously mentioned, there is need to develop and apply Intelligent technologies to protect the corrosion. Because it does not only aim to reduce the cost of maintenances (economic losses), but also protect human from the risk of corrosion during the operational time.

## 2.2 Literature reviews involve with alumina corrosion

Alumina ( $\text{Al}_2\text{O}_3$ ) has considerable potential for extensive usage and applications including coating, part of ceramic material, catalyst and catalyst support. Compared to the other metal oxides, alumina has attached intensive interest because of its fine particle size, good catalytic activity and high surface area. As a result, alumina having these properties is commercially available. Therefore, before conducting experiment, literature review on corrosion behavior of alumina was studied. Generally, it was found that crystalline alumina exists in many metastable phases designed by Greek symbols such as gamma ( $\gamma$ ), delta ( $\delta$ ), eta ( $\eta$ ), theta ( $\theta$ ), kappa ( $\kappa$ ), and chi ( $\chi$ ) before transformation to the stable  $\alpha$ - $\text{Al}_2\text{O}_3$  or corundum which has structure as shown in Figure 2.2.

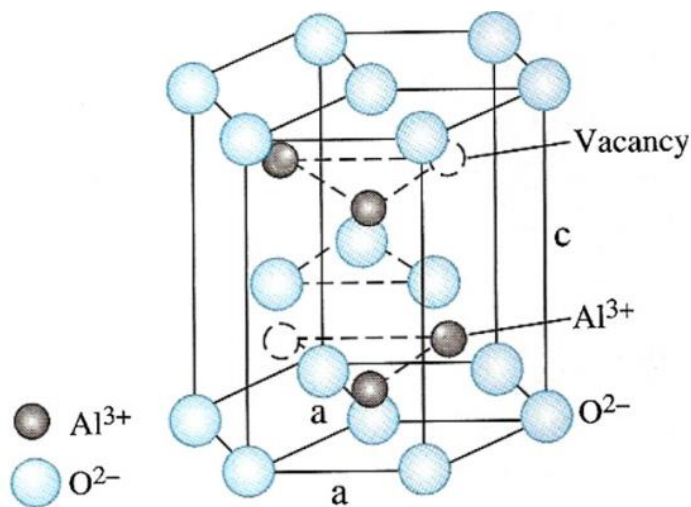


Figure 2.2 A hexagonal close packing of  $\alpha$ - $\text{Al}_2\text{O}_3$  structure [9]

However, the temperature range to transform to alpha-alumina has been reported by a lot of researchers, which involved in nucleation and growth mechanism in sintering process. The phase transformation of alumina was conducted by calcination of alumina precursor. It should be noted that this is an irreversible process; the difference phase transformation sequence is depending on calcination condition, which is resulted from the difference precursor structure. This results in the transformation of different metastable alumina structures toward the stable  $\alpha$ - $\text{Al}_2\text{O}_3$  as shown in Figure 2.3.

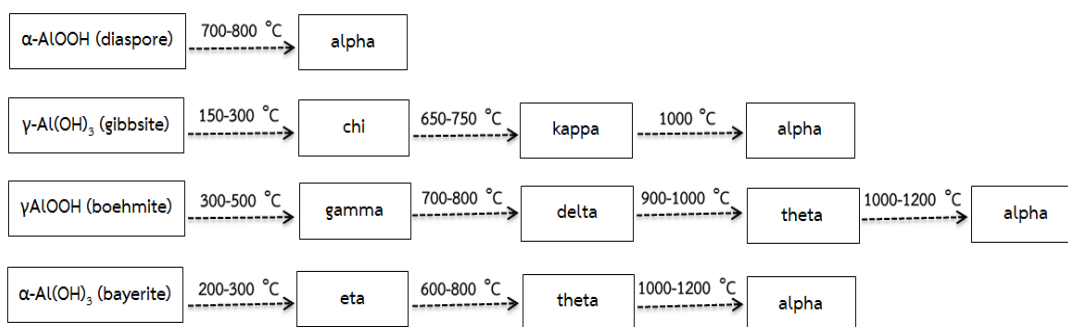
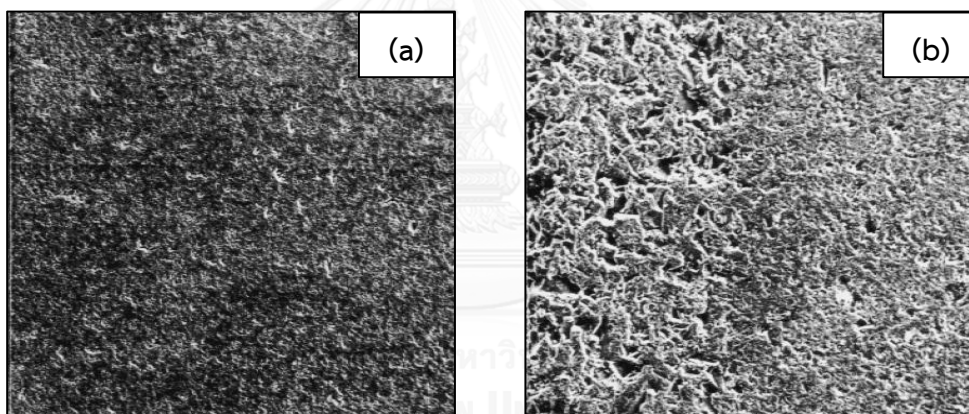


Figure 2.3 Transformation sequences related to metastable to alpha structures [10].

Generally, crystalline alumina has a good corrosion-resistance and chemically inert. However, there are many studies about the corrosion of alumina ceramic at high temperature, highly basic and acidic solution. For example, Oda et al. reported hydrothermal corrosion in different grade of alumina in water under temperature control at 300°C for 10 days, the result was shown that defect formed on surface caused by reaction and dissolution of impurities ( $\text{SiO}_2$  and  $\text{NaO}_2$ ) at grain-boundary of which cross section is shown in Figure 2.4. Moreover, it also concluded that the corroded layer at high impurities content has more thickness than at low impurities content, therefore, the corrosion of alumina ceramic was significantly involved in the impurity level [11].



**Figure 2.4** Cross sectional area of alumina ceramic with (a) low impurities content and (b) high impurities content [11].

Similarly, M. Schacht et al. studied the corrosion of alumina in  $\text{HCl}$ ,  $\text{H}_2\text{SO}_4$  and  $\text{H}_3\text{PO}_4$  aqueous solution at high temperatures (240 up to 500°C) which varied the ratio of impurities particle dispersed on  $\text{Al}_2\text{O}_3$  such as  $\text{SiO}_2$ ,  $\text{TiO}_2$ ,  $\text{MgO}$  and etc. The results in this research are corresponded with the previous conclusion that corrosion resistance depends upon temperature and chemical composition of alumina. The microstructures of alumina in each condition are shown in Figure 2.5 and 2.6.

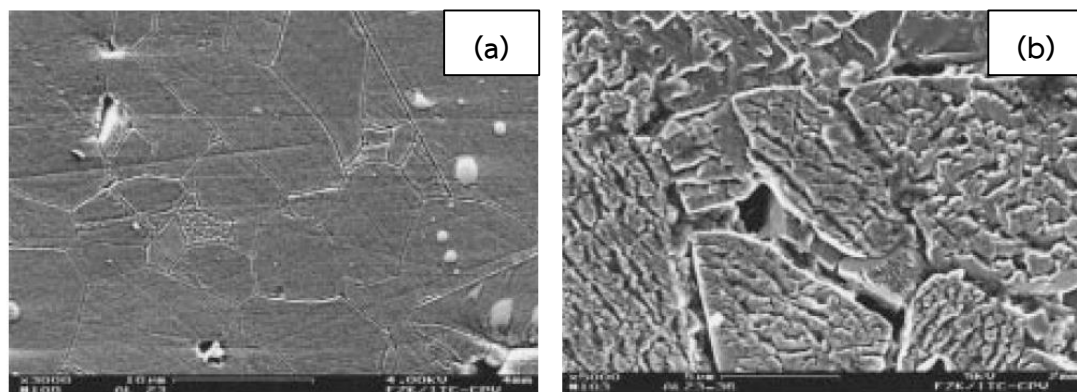


**Figure 2.5** Microstructure of ALC (99.7%  $\text{Al}_2\text{O}_3$ ) (a) before corrosion testing and (b) a corroded layer was formed on surface when exposed to HCl solution [12].

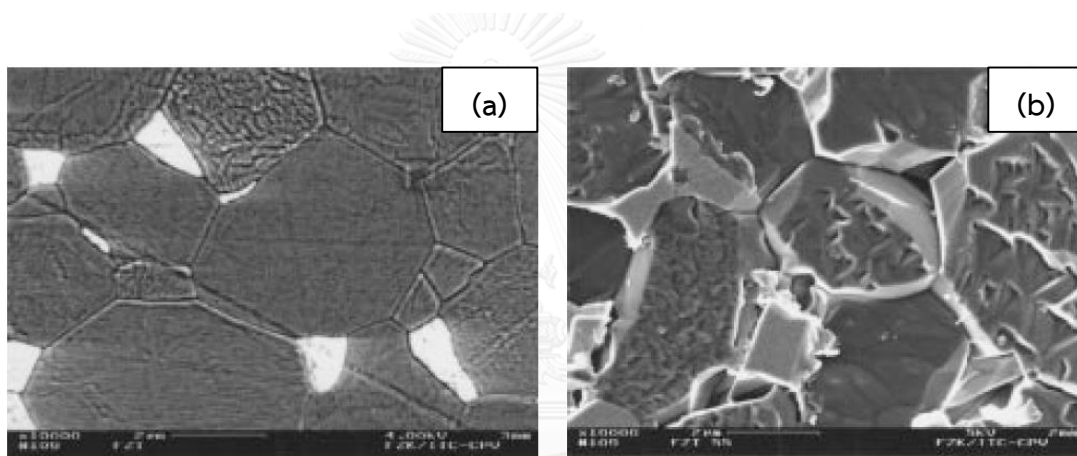


**Figure 2.6** Microstructure of ZTC ( $\text{ZrO}_2+\text{Al}_2\text{O}_3$ ) (a) before corrosion testing and (b) a corroded layer was formed on surface when exposed to  $\text{H}_2\text{SO}_4$  solution [12].

In addition, Figure 2.5 and 2.6 can be summarized that experimental conditions (i.e., corrosive agent, temperature, exposing time and composition at grain boundary) are important factors affecting alumina corrosion as well [12,13].

Sergei M. et al., who reported about influence of environment on delayed failure of alumina. This report should be noted that environmental conditions have a major effect on the microstructure of alumina. The corrosion test was conducted in

various environments which using 99.5 wt% alumina with additive of Mg-O, as can be revealed in Figure 2.7.

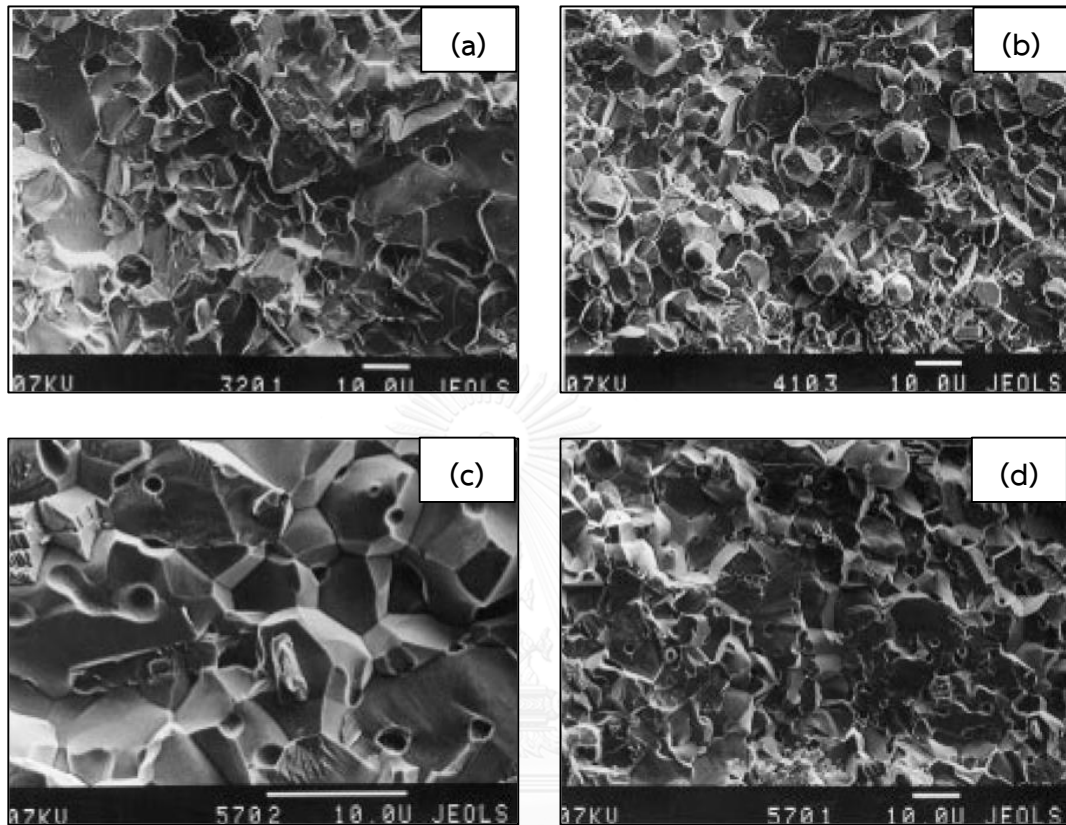


**Figure 2.7** SEM images of alumina after defect was formed on alumina surface tested (a) in air (b) in water and (c,d) in acid at pH = 1 [14].

The result can be concluded that the fracture was found on surface is originated from the interfacial chemical interaction between Mg-O bonding and acid. Additionally, it is directly related to the composition of element and environment conditions, and we can learn that adding Mg-O into alumina can decrease corrosive resistance of alumina ceramics [14].

There are also literature reviews related to corrosion regarding protective film to prevent the corrosion of aluminium. For example, El-Sayed M. et al., studied corrosion inhibition of aluminium in seawater and sodium chloride solution by using electrochemical cell to form passive film on the surface. The experimental result reported that the passive film enable to increase surface charge and protect the charge transfer of aluminium surface, but when aluminium hydroxide is transformed to alumina, it was destroyed by pitting corrosion, which resulted from chloride ions in solution. The corrosion in this process will continue as the reaction with chloride ions progresses and it results in the inhibition efficiency of protective layer is decreasing and eventually the corrosion can form on the surface of aluminum [15].

All of these reviews mentioned above, the corrosion of amorphous alumina in deionized water has not been reported. Therefore, this work is not only aimed to study the corrosion behavior of amorphous alumina in deionized water but also in controlled environments with several adjustable parameters in order to describe the reaction mechanism.

## CHAPTER III

### EXPERIMENTAL

This chapter describes the investigation of alumina corrosion in deionized water. It consists of three main parts; materials, experimental procedure and characterization of the specimens.

#### 3.1 Materials

The materials used in the corrosion tests in deionized water can be divided into two parts including alumina film coated on silicon substrate and  $\text{Al}_2\text{O}_3/\text{TiC}$  substrates, supported by Western Digital Thailand Co., Ltd. The specimens are sputtered with the same process but only changed the substrates in order to ease off some analytical techniques. Typical properties of alumina target used in sputtering process are shown in Table 3.1 and the other metal contaminants are such as Al, Co, Ti, Fe, In, KL, Mg, Ni, Pb, Si, Zr and etc.

**Table 3.1** Typical properties of alumina target.

Property	Value
Purity	99.5%
Grain Size ( $\mu\text{m}$ )	16-22
Temperature of alumina target ( $^{\circ}\text{C}$ )	80
Sputtering thickness ( $\mu\text{m}$ )	1.55
Pressure (mTorr)	20

The specimens are cut into rectangular coupons. In addition, this experiment also using alumina coated on silicon substrate for some characterizations and experimentations which need large size such as X-ray diffraction analysis. These specimens have the shape as shown in Figure 3.1.

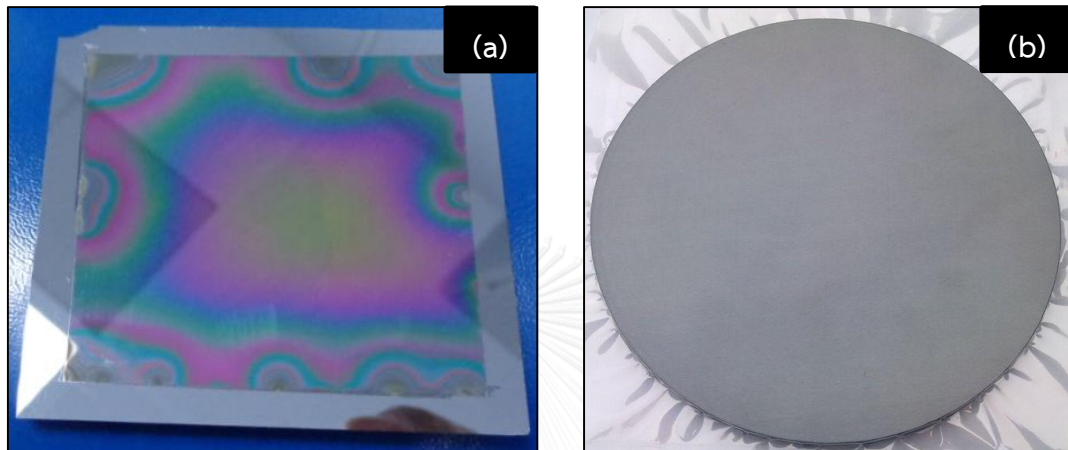


**Figure 3.1** Alumina coated coupons on (a) silicon substrate (b) Al<sub>2</sub>O<sub>3</sub>/TiC substrate.

## 3.2 Experimental Procedures

### 3.2.1 Replication of corrosion in laboratory

Some industries have reported that alumina can be corroded in deionized water at low temperature. In this preliminary study, it needs to replicate the corrosion on the specimens to make sure that it is possible to see the defect formed on the surface. Before corrosion testing, specimens are thoroughly washed with isopropyl alcohol (IPA) and distilled water. Then, cleaned specimen is placed into a beaker filled with deionized water. Target temperature is adjusted by heating the system with hot plate as shown in Figure 3.2.

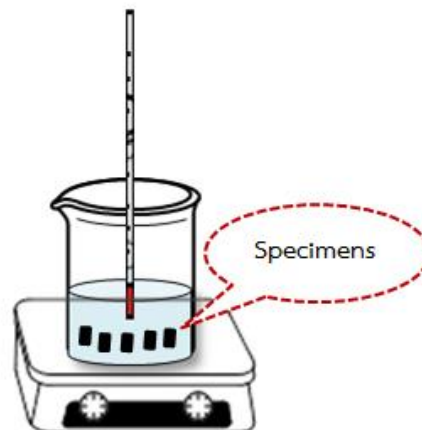


**Figure 3.2** The corrosion tests of alumina ceramics in deionized water.

Corrosion tests were conducted at temperature range of  $25^{\circ}\text{C}$  to  $80^{\circ}\text{C}$  with various immersion time. All conditions are fixed as following;

- At temperature of  $25^{\circ}\text{C}$ , the investigations were conducted in the range of 60 to 240 minutes of immersion time.
- At temperature of  $40^{\circ}\text{C}$ , the investigations were conducted in the range of 30 to 180 minutes of immersion time.
- At temperature of  $50^{\circ}\text{C}$ , the investigations were conducted in the range of 30 to 90 minutes of immersion time.
- At temperature of  $60^{\circ}\text{C}$ , the investigations were conducted in the range of 15 to 60 minutes of immersion time.
- At temperature of  $80^{\circ}\text{C}$ , the investigations were conducted in the range of 15 to 60 minutes of immersion time.

After the tests were completed, the specimens were removed from the beakers, rinsed with distilled water and dried at room temperature. The microstructure of the surface and cross-section for corroded specimen was examined by scanning electron microscopy (SEM) and the phase transformation of the specimen was examined by X-ray diffraction (XRD).

### 3.2.2 Experimental apparatus involved in alumina corrosion test

#### 3.2.2.1 Apparatus for studying the effect of hydroxyl radicals in water.

The corrosion test in this part was performed at the temperature of 50 °C and immersion time of 30, 60 and 90 minutes respectively. The specimens were put into deionized water and used the VUV (Vacuum Ultra Violet) lamp as the light source, which has a high potential to generate the hydroxyl radicals. The schematic diagram is shown in Figure 3.3.

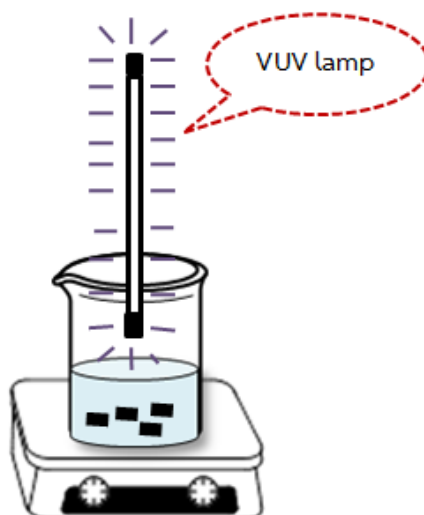


**Figure 3.3** Experimental set-up for the hydroxyl radical testing.

### 3.2.2.2 Apparatus for studying the effect of pH of water.

This experiment was conducted in deionized water which various pH in very extreme condition (strong acid and strong alkaline solution). The solution was adjusted by hydrochloric acid (HCl) or sodium hydroxide (NaOH). The pH was set at 4, 7 and 9 in the temperature of 50 °C, the variation period of time at 30, 60 and 90 minutes. The experimental design is shown in Figure 3.4.

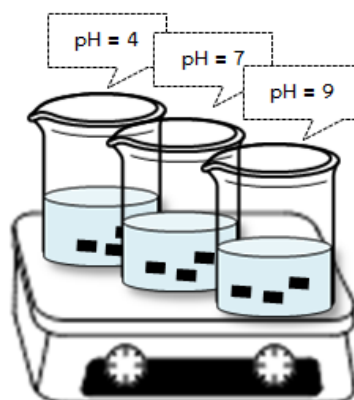


**Figure 3.4** Experimental set-up for studying the effect of pH.

จุฬาลงกรณ์มหาวิทยาลัย  
CHULALONGKORN UNIVERSITY

### 3.2.2.3 Apparatus for studying the effect of oxygen content in water.

In this experiment, the specimens were put in deionized water that was heated in two conditions; (i) at the temperature of 50°C for 30 and 90 minutes and (ii) at the temperature of 60°C for 15 and 50 minutes. This test was proposed to investigate the effect of oxygen content which may cause the defect. The test in this session has a diagram as shown in Figure 3.5. Oxygen content in deionized water was measured by Oxyguard equipment, and varied by four different kinds of water treatments as follows.

- Deionized water that was continuously purged nitrogen gas to remove dissolved oxygen throughout the experiment. This system contains the oxygen content is about 5% of the solubility.
- Deionized water directly obtained from using Milli Q system (Millipore) which is normal DI water and has the oxygen content is about 48% of the solubility.
- Deionized water that was boiled and cooled down to room temperature. This system contains the oxygen content is about 60% of the solubility.
- Deionized water that was continuously purged air to increase oxygen content in water throughout the experiment. This system contains the oxygen content is about 96% of the solubility.

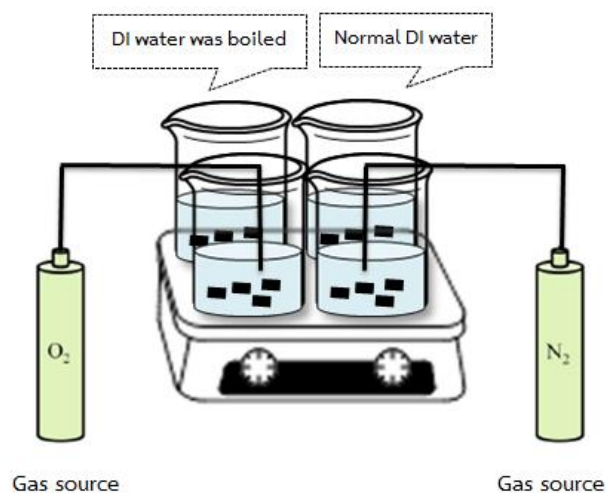


**Figure 3.5** Schematic diagrams for studying the effect of oxygen content in water.

#### 3.2.2.4 Apparatus for studying the effect of ions in water.

The study of ions in water was done by adding some cations and anions into the solution. Therefore, in this part, deionized water was varied kinds of cations (such as  $\text{Al}^{3+}$ ,  $\text{Mg}^{2+}$  and  $\text{Zn}^{2+}$  ion) and anions (such as  $\text{Cl}^-$ ,  $\text{Br}^-$ ,  $\text{NO}_3^-$ , and  $\text{PO}_4^{3-}$ ) with the concentration in the range from 20 to 500 ppb. This experiment was conducted by immersing the specimen into water at 50 °C for 30, 60 and 90 minutes as shown in Figure 3.6.

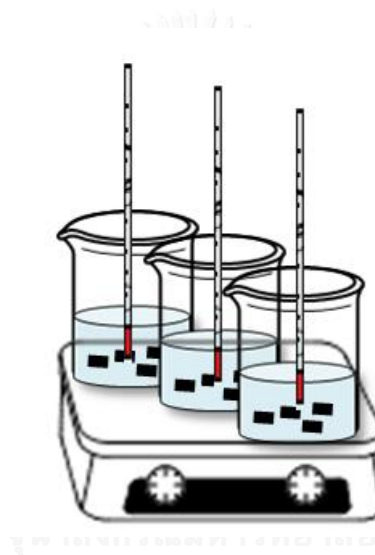


**Figure 3.6** Experimental setup for studying effect of ions in water testing.

#### 3.2.2.5 Apparatus for studying the effect of electron transfer.

In this part, the corrosion was tested to investigate effect of electrons transfer on the formation of defect. The experimental setup is shown in Figure 3.7. In the experiment, two specimens were tested simultaneously. The specimen was attached to one electrode of a DC power supply, while another one of electrode was connected with metal. Together with one specimen was connected to the positive electrode and another was connected to negative electrode, the power supply to

the specimen was varied in the range of 6 to 25 volt. All of specimens were immersed into deionized water in 2 conditions; (i) at the temperature of 50°C for 30 and 60 minutes and (ii) at the temperature of 60°C for 15 and 50 minutes. Additionally, the bottom of beaker was also contained a specimen without connecting with any electrode as a control the experiment.

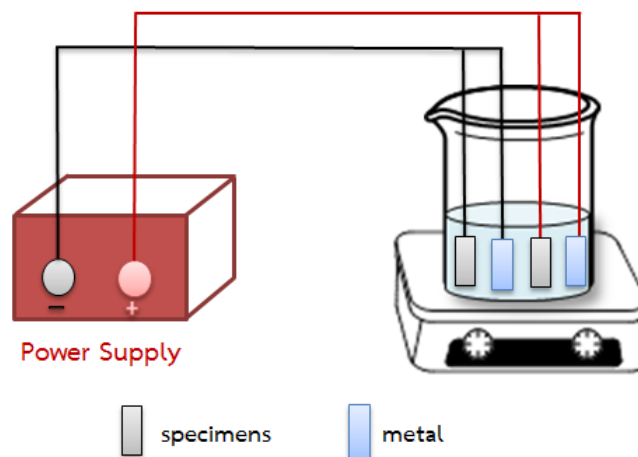


**Figure 3.7** Experimental set-up for the investigation the effect of electron transfer on corrosion of alumina.

จุฬาลงกรณ์มหาวิทยาลัย  
CHULALONGKORN UNIVERSITY

### 3.2.2.6 Apparatus for studying the effect of the local concentration of $H^+/OH^-$ .

In this experiment, the corrosion testing was proposed to investigate the effects of distance from surface charge to the electrode in which a lot of previous reports have mentioned that the distribution of the concentration of ion is changed when the distance between surface charges is changed as well. The experimental set-up is shown in Figure 3.8. The metal which was stainless steel connected with power supply in both positive and negative charge. The specimens were hung on the pole in different distance with DI water as an electrolyte solution. The AlTiC coupons

were hung in four distances, at the positive electrode as same as the negative electrode including 1 and 10 millimeters. Additionally, one of coupon also put into the solution without connecting to electrode which used as a control. This corrosion testing was conducted at the temperature of 50°C for 30 and 60 minutes of the exposing time, the potential was varied from power supply in the range of 3 to 15 volts.

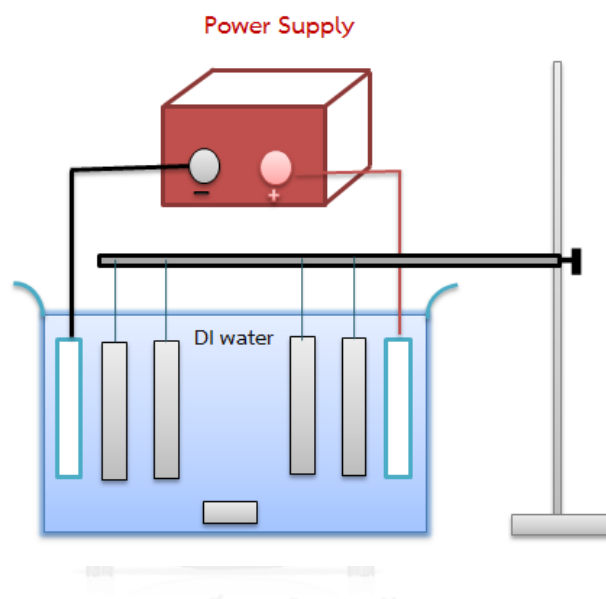


**Figure 3.8** Experimental setup for investigation the effects of the local concentration of  $H^+/OH^-$  in water.

### 3.2.2.7 Apparatus for studying the effect of electron transfer couple with oxygen content.

In this section, the experiment intends to investigate the effect of electron transfer couple with oxygen content simultaneously. The diagram of equipment was setup to be like the studying effect of electron transfer session, but this experimental does not use the metals are electrode. The two specimens were directly attached to positive and negative electrode of power supply. This system was varied the amount

of dissolved oxygen in two conditions; (i) increasing oxygen content by continuously bubble air into DI water and (ii) decreasing oxygen content by continuously purging nitrogen gas as well. In addition, this session still uses one of specimen put into DI water as a control. Corrosion testing was conducted at the temperature of 50°C for 30 and 60 minutes, and using the electrical potential was varied at 3 and 6 volts. The schematic diagram is shown in Figure 3.9.

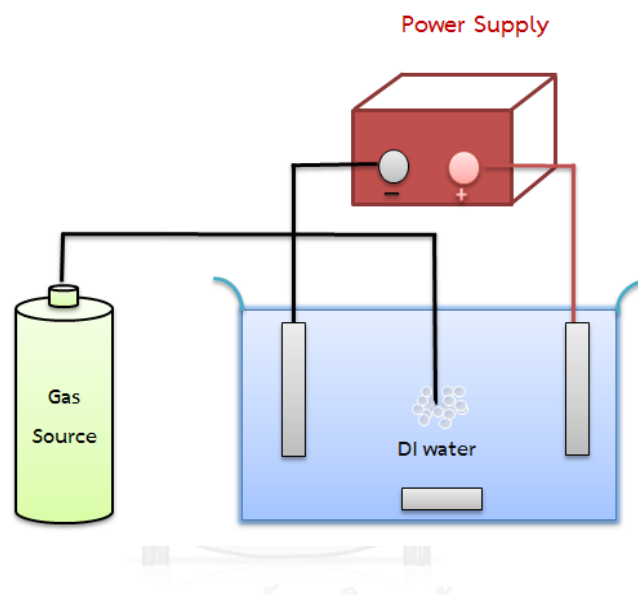


**Figure 3.9** Experimental set-up for investigation of the effect of electron transfer couple with oxygen content.

### 3.3 Characterizations

#### 3.3.1 Scanning Electron Microscopy (SEM)

Morphology of the obtained product was investigated by a field emission scanning electron microscope (MERLIN-Analytical Power for the Sub-Nanometer World), in which a special property is high resolution imaging of non-conductive materials through charge compensation. The FE-SEM is operated in secondary mode with extra-high tension (EHT) supplies at 1.00 kV at Western Digital Thailand Co., Ltd.

#### 3.3.2 X-ray diffraction (XRD)

X-ray diffraction analytical technique is useful for providing structural information about the crystalline phase and chemical compounds of the specimens (XRD, Bruker AXS, Difraktometer D8) with a  $\text{CuK}\alpha$  radiation source at 40 kV and wavelength equal to  $1.5406 \text{ \AA}$ . The measurement was carried out in the range of  $2\theta = 10^\circ - 60^\circ$  at Department of Materials Science, Chulalongkorn University.

#### 3.3.3 Fourier Transform Infrared spectroscopy (FTIR)

The functional groups of the specimens were identified by a Fourier transform infrared spectrometer (Nicolet 8700) at Western Digital Thailand Co., Ltd. The infrared spectra were recorded between wavenumber of  $400\text{-}4000 \text{ cm}^{-1}$ . Before measuring, surface area of silicon coupons were scraped out and mixed with KBr while a lot of  $\text{Al}_2\text{O}_3/\text{TiC}$  coupons are directly detected by ATR-FTIR, which used for measurement the peak height after defect formation on the specimens.

### 3.3.4 Time of Flight Secondary Ion Mass Spectrometry (ToF-SIMS)

The surface chemistry and the distribution of ions on surface specimen can be determined by Time of Flight Secondary Ion Mass Spectrometry (ToF-SIMS) which is a highly sensitive technique. The analytical tests were performed with a PHI's TRIFT III system. The specimen is cut into square shape (500mmx500 mm) and operated under 25 KeV Ga<sup>+</sup> ion beam bombardment with unbunched mode at Western Digital Thailand Co., Ltd.

### 3.3.5 Point of zero charge determination

The point of zero charge (abbreviated as PZC) of amorphous alumina that used in this research was determined by titration method [16] which was carried out with 0.1 mol dm<sup>-3</sup> KNO<sub>3</sub> solution. The 50 ml of KNO<sub>3</sub> solution was poured into 250 ml of volumetric flasks. The initial pH values of the solution are adjusted from 2 to 10, by using 0.1 N HNO<sub>3</sub> or NaOH, the total volume of the solution in each flask is made up exactly to 50 ml by adding the KNO<sub>3</sub> solution of the same concentration. Then, the initial pH values of solution are accurately noted. Thirty-gram of the alumina-coated coupon is added to each flask and the flask is capped immediately. After that, the suspension is constantly shaken to equilibrate for 48 hours in a shaker bath at 25 °C with the rotational speed at 120 rpm. When the shaking was completed, the final pH values of the supernatant liquid were recorded. The difference between initial and final pH values ( $\Delta\text{pH}$ ) was plotted versus the initial pH values. The PZC value is calculated from the intersection of graph at which  $\Delta\text{pH}$  is zero, gave the PZC.

## CHAPTER IV

### RESULTS AND DISCUSSION

In this research, characterizations on alumina were sputtered onto coupons by sputtering process need to be investigated. The replication of defect on alumina coated-coupon was preliminarily studied and described. In addition, the factors affecting the alumina corrosion are also mentioned in this chapter. These results will leads to propose the ways to prevention of the problem.

#### 4.1 Characterizations on alumina-coated coupon

In order to understand about corrosion behavior, the characterization of alumina-coated coupon is needed. Because this research is focused on the alumina which is the solid phase. Therefore, in this session, the structural composition, phase transformation and the functional group that take place on alumina were investigated. As for the liquid phase, it is not significantly changed that can be ignored. The characterization on alumina-coated coupon is divided into two parts as following.

##### 4.1.1 X-ray diffraction analysis

In this experiment, the specimen which is alumina-coated coupon on silicon substrate (as shown in Figure 4.1a) was used in order to reduce the interfering signal between the considered  $\text{Al}_2\text{O}_3$  thin film and  $\text{Al}_2\text{O}_3$  signal which comes from alumina

embedded in the substrate. The specimens were identified by X-ray diffraction (XRD) analysis. One of the specimens was subjected to this analysis without heating process. In order to verify the XRD result, the specimen was heated at the temperature of 1000 °C with heating rate of 20 °C/min for 2 hours before conducting to XRD again. The results of XRD analysis are shown in Figure 4.1.

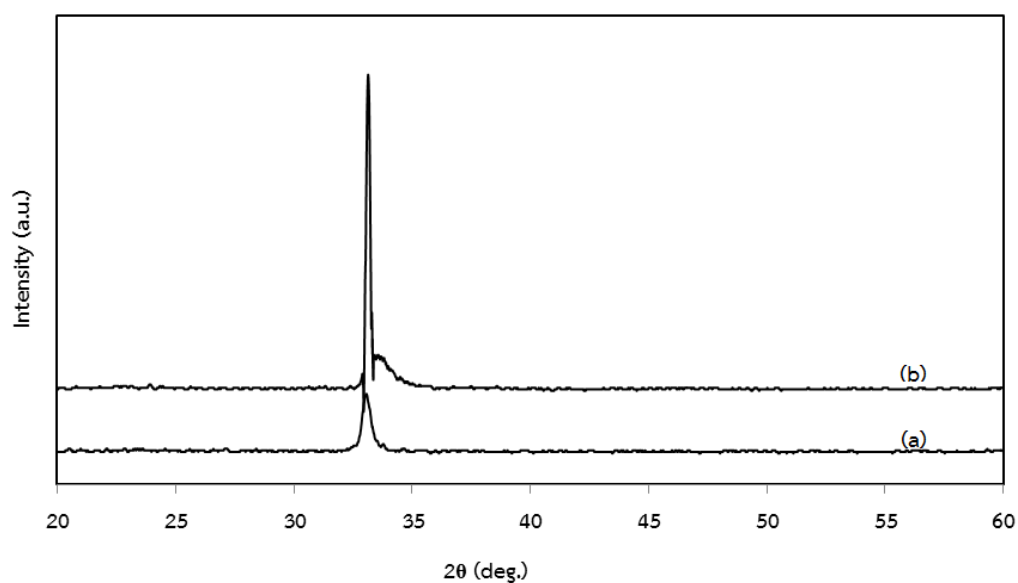


**Figure 4.1** The XRD patterns of alumina-coated coupons on silicon substrate. (a) the pattern of deposited state (b) the pattern after heat treatment

The preliminary results of XRD measurements for alumina-coated coupons before and after heat treatment revealed that both conditions have the similar peak position of silicon at  $2\theta \sim 33^\circ$ . None of alumina peak showed in this pattern. This occurrence may be a result of the very thin alumina film which is coated on the surface or may be the result of the amorphousness of that alumina. Moreover, a significant change in diffraction pattern is detected after heat treatment only. This pattern shows a broad peak at  $2\theta \sim 33.5^\circ$ , but it cannot match to any form of alumina or silicon oxide though the phase transformation to crystalline alumina should be

found after heat treatment at more than 700°C. Therefore, it is possible that the other compositions may occur on alumina surface but it cannot be detected by XRD method. In addition, it can be predicted that the alumina thin film on the coupons, coated by sputtering process, is indubitably amorphous. As a result, it has the chance to be more reactive than the crystalline structure.

#### 4.1.2 Fourier transform infrared spectroscopy analysis

This technique has been examined to identify the functional groups of the specimen both before and after the defect was formed on surface. Basically, each functional group has different characteristic and infrared absorption, which undergoes change in vibration modes. In this session, the coated layer of  $\text{Al}_2\text{O}_3$  is scraped out from the specimen and mixed with potassium bromide (KBr) before subjecting to FTIR analysis and detected in transmission mode, the obtained result is shown in Figure 4.2.

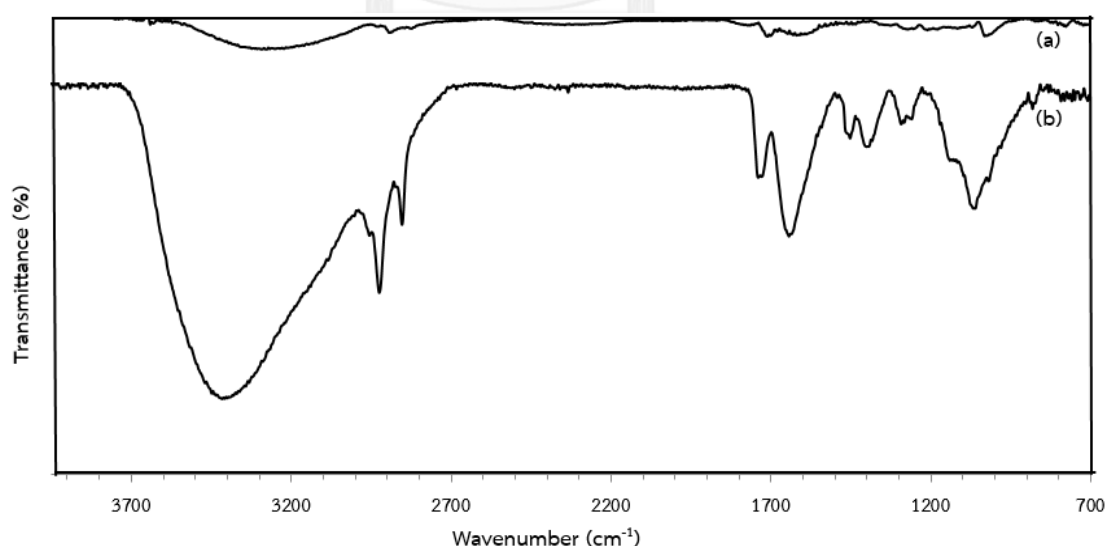


**Figure 4.2** FTIR transmittance spectra of alumina-coated coupons. (a) the alumina-coated coupons grown on Si-substrate (b) the spectra of alumina-coated coupons after the defect formed on the alumina surface.

The FTIR results indicated that the main functional group of alumina thin film is the O-H stretching vibration at wavenumber around 3200-3500  $\text{cm}^{-1}$  [17]. For the comparison, one of the alumina-coated coupons immersed in DI water at the temperature of 50°C for 60 minutes is investigated as well. The defect of the specimen is detected by SEM. Then the corroded layer is analyzed by FTIR. The O-H stretching band is clearly observed when the defect formed on the alumina surface (see in Figure 4.2b). This peak may result from the formation of defect on the surface. In other words, this result suggested that the hydrolysis reaction of amorphous alumina is the major cause of the defect. The rest of the peaks correspond to the stretching vibration of C-H at 3000-2850  $\text{cm}^{-1}$ , C=O bonding appears in the range 670-1640  $\text{cm}^{-1}$ . These peaks may be resulted from the contamination during the corrosion testing.

From the FTIR results, it can be concluded that the corroded layer on the surface is caused by OH- group in DI water. This OH group can be reacting with amorphous alumina, which is hypothesized that it is hydrolysis reaction.

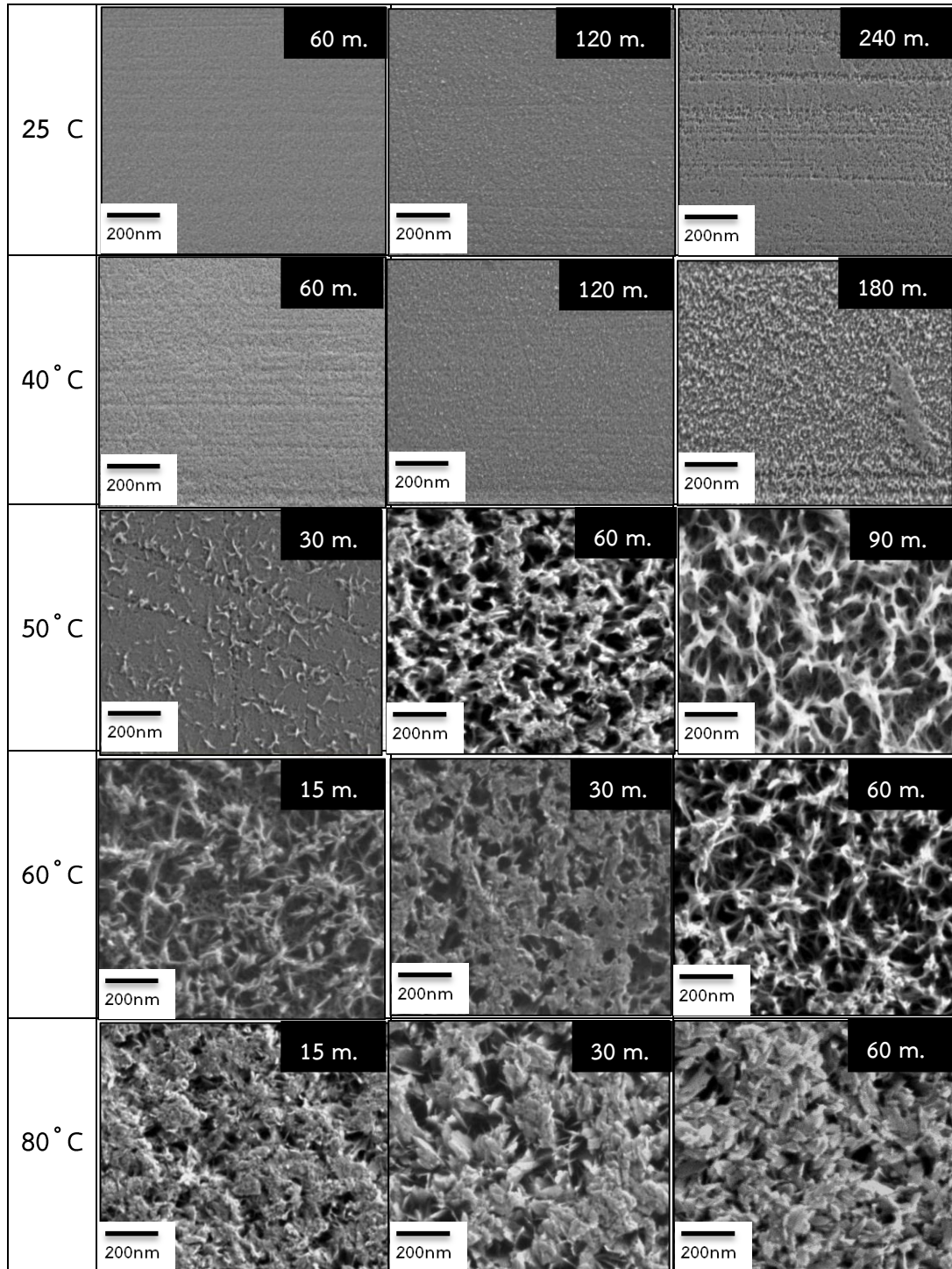
#### **4.2 Replication the corrosion of amorphous alumina in laboratory**

In order to verify whether the defect observed on the specimen surface is the same as the defect on the surface of the crystalline alumina as seen in general researches or not, the replication of the corroded amorphous alumina is needed. The factors which effect to the alumina corrosion in DI water are investigated. However, the weight loss due to the corrosion on the surface of alumina specimens in this work did not consider because the alumina layer is very thin and gives to the non-significantly difference in weight.

Firstly, the defect on the alumina surface in laboratory has to be replicated. Since all of the researchers have reported about crystalline alumina, but the corrosion of amorphous alumina has not been well understood. So, it is important to investigate the corroded amorphous alumina in order to ensure that the defect is really formed on the surface. The corrosion test was conducted at the temperature in the range of 25 to 80°C with various conditions as mentioned in previous chapter. The results are shown in Table 4.1.



**Table 4.1** SEM results after the corrosion tests.



Each corrosion tests are repeated many times. The results indicated that no defect formed at temperature in the range of 25°C to 45°C although each specimen is immersed in DI water for a long period of time. Moreover, this experiment can be concluded that the temperature at 25°C and 40°C may not be the starting temperatures that cause the corrosion of amorphous alumina. From the SEM results, they can also be concluded that the defect becomes apparent at temperature 50°C, immersion time for 60 minutes (for the immersion time as 30 minutes, the defect is not clearly observed). These defects tend to increase when the immersion time is prolonged. Especially, the severe level of the defect is formed on the surface of specimens at the temperature 60°C to 80°C s although they are immersed in DI water in short period of time.

From the results mentioned above, the cross-sectional area of the full-defected specimens needs to be investigated. The result is shown in Figure 4.3.

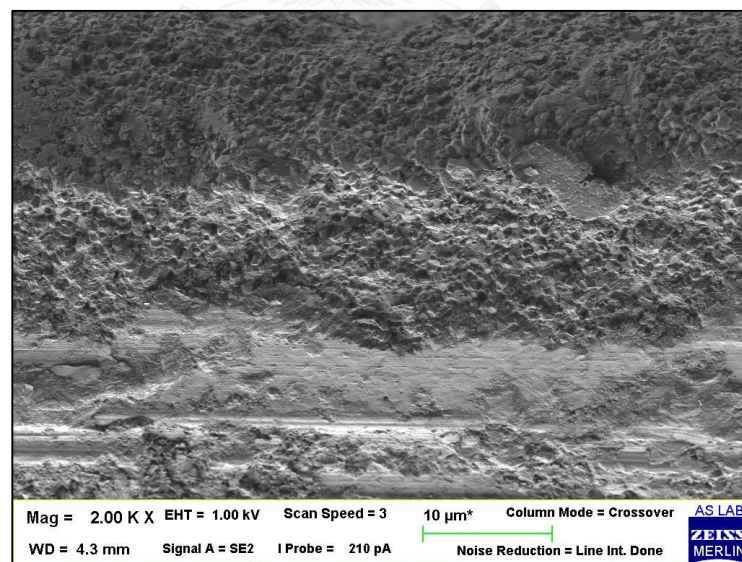


**Figure 4.3** Cross-sectional area of the specimen at 2.00KX magnification.

Initially, the experimental result in Figure 4.3 indicates that the defect seems to protrude from the surface specimen. However, the results from SEM analysis are

not enough to confirm the defect formation due to the lack of the reference line to identify the original surface. The specific instrument such as Atomic force microscopy (AFM) should be used in order to confirm the results in this section again.

In addition, the average particle size of the defect formed on surface (as shown in Table 4.1) is also measured by Image Processing 6.0 plus program. In order to explain the corrosion mechanism of amorphous alumina in quantitative and confirm the defect level obtained from SEM images, the particle size is measured as shown in Table 4.2.

**Table 4.2** The average particle size of the formation of the defect on amorphous alumina.

Temperature (°C)	Average particle size of the defect (nm), when the specimen was immersed in DI water for various period of time.					
	15 min	30min	60 min	90 min	120 min	180 min
25	-	-	0	-	0	0
40	-	-	0	-	0	0
50	-	40.07	106.24	114.44	-	-
60	82.47	114.06	149.50	-	-	-
80	93.13	147.35	181.25	-	-	-

According to the Table 4.2, it should be noted that the formation of the defect has a large size when the temperature and immersion time is increased. The characteristic of the defect formed on the surface has lots of level, which based on the particle size. From the result of Image Processing 6.0 plus Program, it can be concluded that if the average particle size is smaller than 106.24 nanometers, the

defect is not severe level and can be accepted. In contrast, if the average particle size is larger than 106.24 nanometers, it will be considered as not acceptable (this criterion can very depend on the acceptable value of each industry).

Moreover, the height of OH peak (hydroxyl group) of all specimens (as reported in Table 4.1) are also investigated by using ATR-FTIR in order to compare the amount of hydroxyl group, which is used to identify the defect formed on the alumina surface. Additionally, the ATR-FTIR is used to indicate whether the temperature and exposure time affect to the surface defect or not. All of the measurements are detected at the center of the specimens for two times. The height of OH peak at wavenumber about  $3200\text{-}3500\text{ cm}^{-1}$  is recorded. The manner of measurement is shown in Figure 4.4. The more intensity of the peak height has, the greater amount of OH functional group will be.

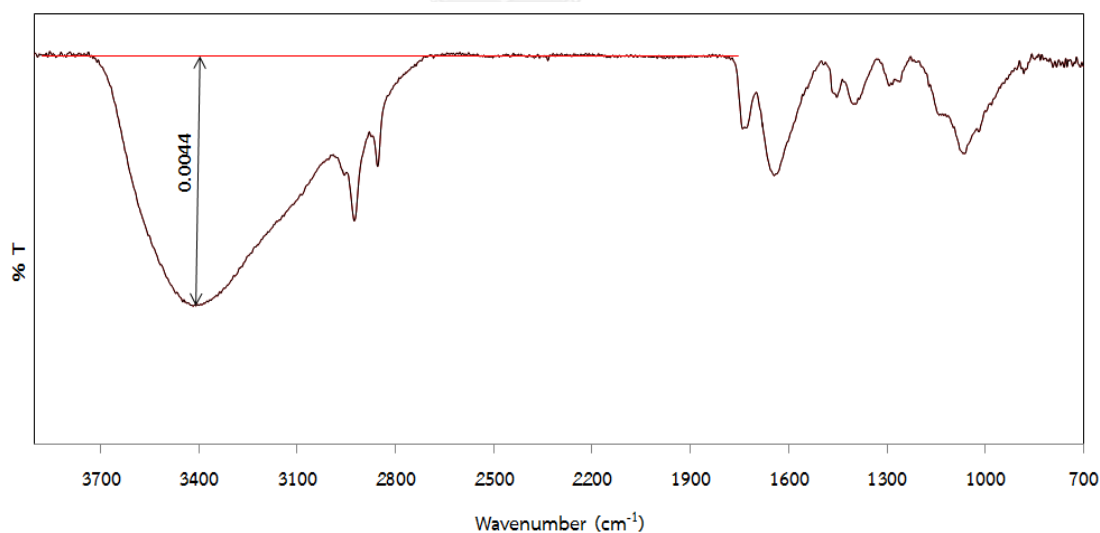


**Figure 4.4** Example of the OH peak height measurement analyzed by ATR-FTIR at the temperature of  $50^{\circ}\text{C}$  for 60 minutes.

The relationship between OH peak height and immersion time is plotted as shown in Figure 4.5. Since there is no defect found on the surface specimen at room temperature, the beginning temperature in the experiments is started at 40°C. In this condition, the O-H signal cannot be detected O-H signal by ATR-FTIR. It is difficult to distinguish clearly at this temperature. This result may be occurred because of the amount of alumina coating on the surface being too small.

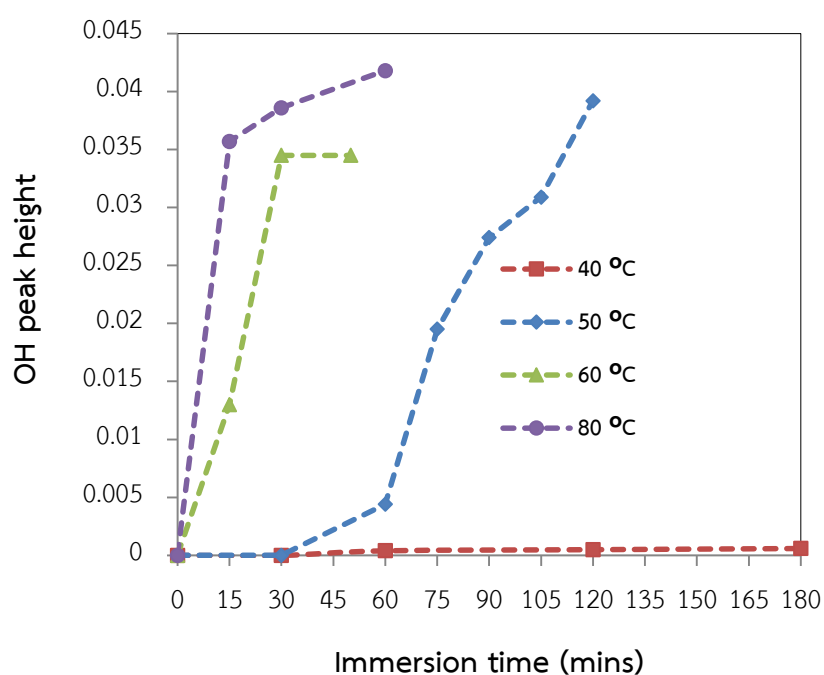


**Figure 4.5** The correlation between the OH peak height and the immersion time in each condition.

From Figure 4.5, it should be noted that the amount of OH peak tends to be increased when temperature was increasing. The intensity of OH group was increasing when the defect is much greater. The relationship among the signals directly related to the amount of OH group formed on the specimens. The initial slopes of each temperature are likely to be linear at the initial stage and continuously declined after that. The defect cannot be found at low temperature (40°C) and cannot detect the

OH signal by ATR-FTIR. The rate of the reaction is negligible, which is complied with the results previously observed. Therefore, this study can be used to confirm that the corrosion of amorphous alumina is caused by hydrolysis reaction.

### 4.3 Factors affecting the corrosion of amorphous alumina

The purpose of this research is to study the corrosion susceptibility of Al<sub>2</sub>O<sub>3</sub> thin film in water. The preliminary result was assumed that it might be associated with many factors which are described below.

#### 4.3.1 The effects of OH radicals

The purpose of this experiment is to verify whether or not the OH group affects the defect formation on alumina surface. From the previous reports, it had been recognized that the OH radicals (OH<sup>•</sup>) are more reactive than the OH group. This corrosion testing is designed by intentionally increase the reactivity of OH ions. The simultaneously vacuum ultra violet (VUV) radiation applying is done. The OH ions change into OH radicals by water dissociation. Therefore, when the specimen is immersed in DI water, the chance of defect formation on the surface is higher to form. The VUV light (at wavelength 184 nm) causes photolysis reaction [18] because of the degradation of water, as shown in the following equation (1)



In this part, the corrosion testing is only performed in two conditions, using the same period of time as previous session but different in the temperature ( $40^{\circ}\text{C}$  and  $50^{\circ}\text{C}$ ). If the OH group has the effect on this corrosion, the defect would be formed at low temperature (less than  $50^{\circ}\text{C}$ ). The results are shown in Figure 4.6 and 4.7.

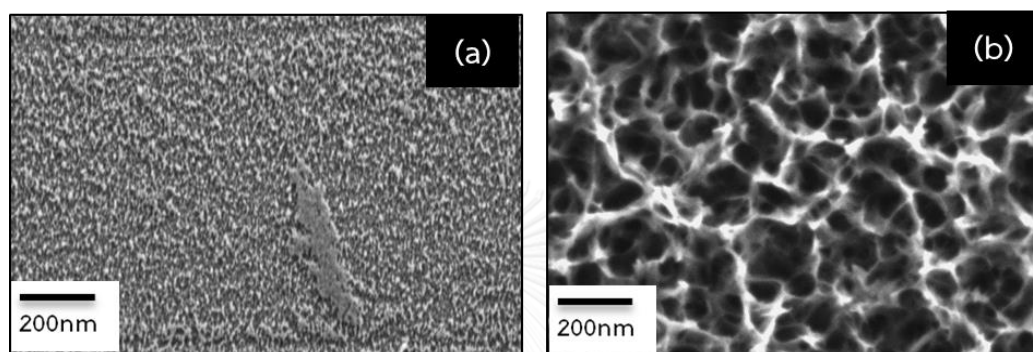


**Figure 4.6** SEM images of the specimens shows the result of the surface corrosion after the specimen is immersed in DI water at  $40^{\circ}\text{C}$  for (a) 180 minutes without irradiation and (b) 150 minutes with VUV irradiation.

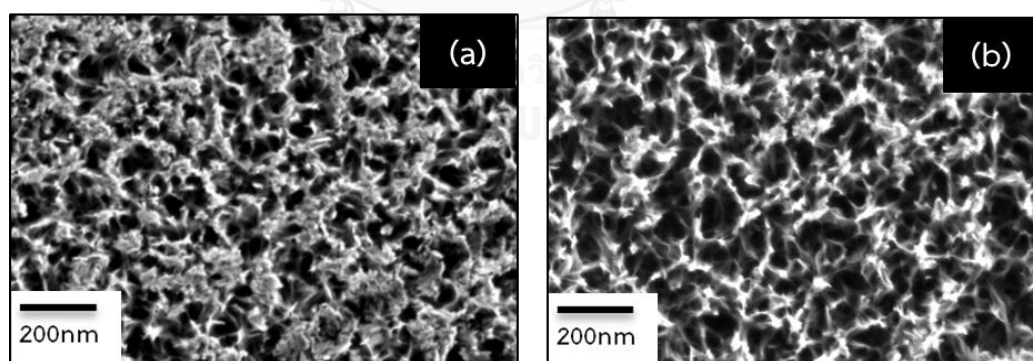
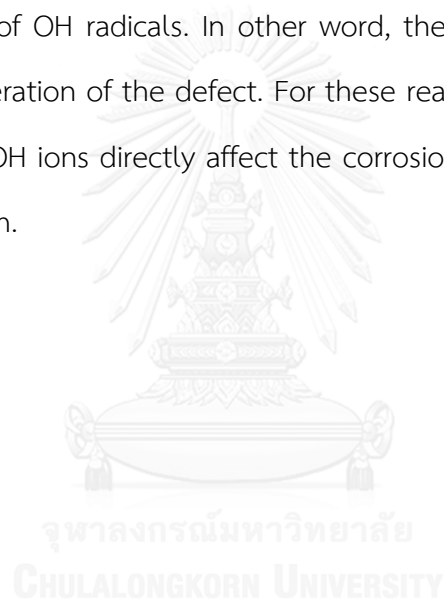


**Figure 4.7** SEM images of the specimens shows the result of the surface corrosion after the specimen is immersed in DI water at  $50^{\circ}\text{C}$  for 60 minutes (a) without irradiation and (b) with VUV irradiation.

The SEM results indicated that at the condition 40°C, immersion time 150 minutes, the defect is formed on the surface specimen. In contrast, the result showed in Figure 4.6(a), can be seen that no surface defect occurred even the specimens are immersed in DI water at 40°C for 180 minutes. However, the experimental result at temperature of 50°C for 60 minutes, the particle size is measured again, it is also found that particle size of the defect is 174.88 nanometers, which is greater than the particle size of the specimen from non-irradiation condition (as shown in Table 4.2). Therefore, it can be concluded that the defect tends to form easily by the attack of OH radicals. In other word, the generation of OH radicals in water leads to acceleration of the defect. For these reasons, it can be leading to the conclusion that the OH ions directly affect the corrosion behavior of the amorphous alumina in this system.



### 4.3.2 The effect of water pH

This section is still focusing on the effect of hydroxyl group concentration in DI water. Generally, it is well known that the hydroxyl concentration at high pH value (alkaline solution) is higher than that at low pH value (acidic solution). This experiment is conducted under the hypothesis that if the hydroxyl group causes the defect formation, the defect will be more observed on the surface after the specimen had immersed in high pH water. The hypothesis is represented in Figure 4.8.

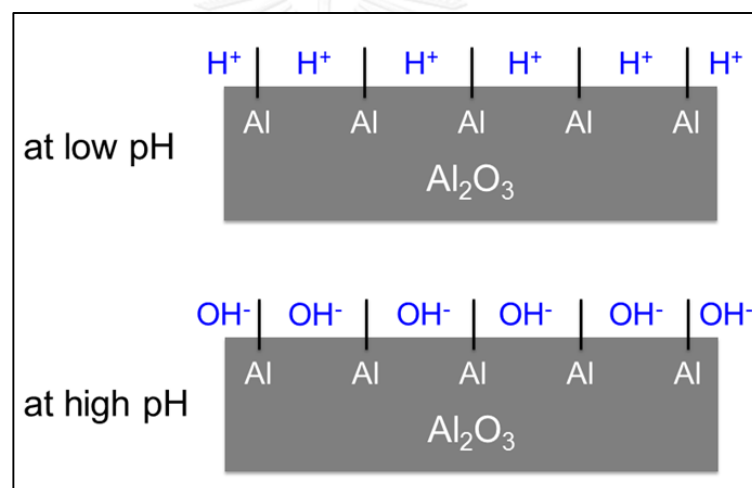


**Figure 4.8** The hypothesis for surface charge of the specimen when immersed in DI water at low and high pH, respectively.

In this study, the specimens are immersed in DI water which has pH values 4, 7 and 9 in order to confirm the hypothesis as mentioned above. The corrosion tests are repeated several times. The result is shown in Figure 4.9 to 4.11.

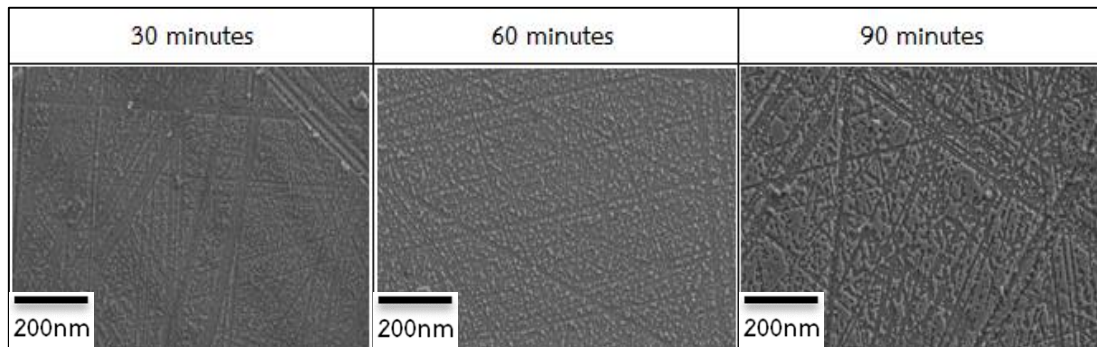


**Figure 4.9** SEM images of the specimens after the specimen is immersed in DI water at pH of 4 with various period of time.

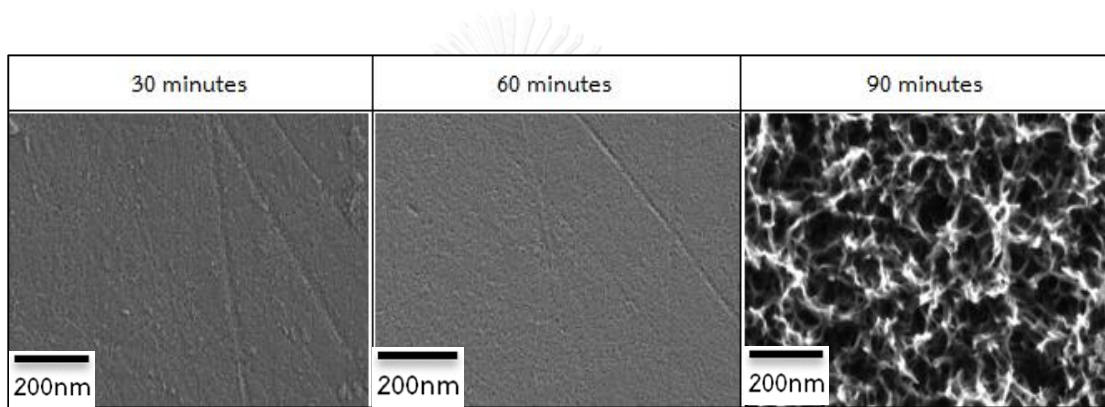


**Figure 4.10** SEM images of the specimens after the specimen is immersed in DI water at pH of 7 with various period of time.

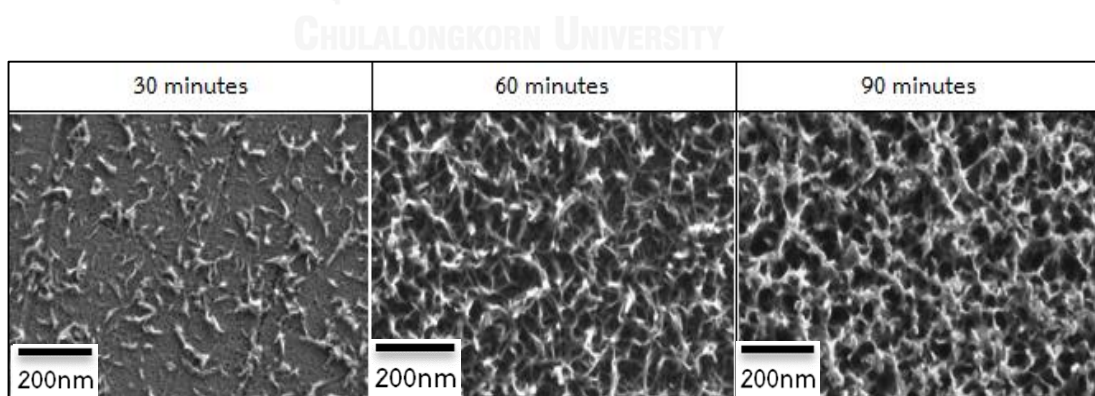


**Figure 4.11** SEM images of the specimens after the specimen is immersed in DI water at pH of 9 with various period of time.

From The results in Figure 4.9 to 4.11, they can be indicated that the defect did not see at pH of 4 even the immersion time is longer than 90 minutes. The defect begins to form on the surface at pH of 7. On the other hand, all of the specimens are found with corroded layer at pH of 9, in which the concentration of hydroxyl is increased. The results respond with the hypothesis that the corrosion of amorphous alumina is the result from  $\text{OH}^-$  ion in DI water.

Moreover, the point of zero charge (PZC) of amorphous alumina also determine in this session. Each metal oxide has a different of PZC. For example;  $\text{Al}_2\text{O}_3$ ,  $\text{SiO}_2$  and  $\text{TiO}_2$  have their own charge associated on the surface. The change in functional group on the specimen surface which respect to the pH of the solution is shown in Figure 4.12. For these reasons, the PZC should be determined in order to support the result from the study on the effect of pH of solutions.

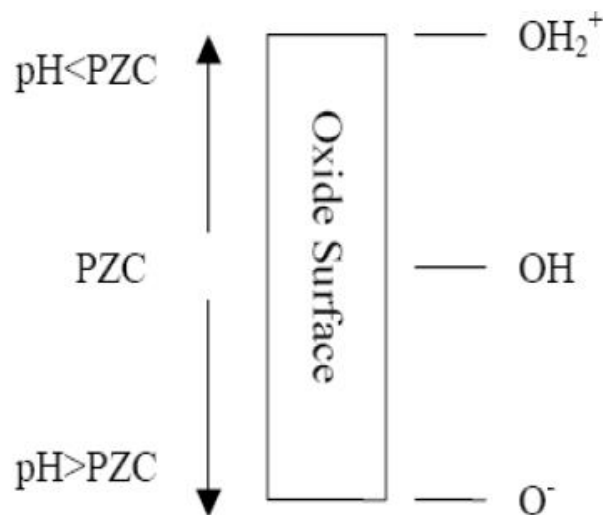


**Figure 4.12** The point of zero charge model for metal oxide. [19].

From the Figure above, when the material is submerged in the solution that has pH equal to PZC, the surface sites had no charge. If the pH value is lower than the PZC, the charge on the surface sites will be positively charged ( $\text{Me-OH}^+$ ). In contrast, if the pH value is higher than the PZC, the surface sites will be negatively charged ( $\text{Me-OH}^-$ ). According to the theory, the graph intersection on the horizontal axis is PZC. In this research, the PZC of amorphous alumina can be obtained from the titration method which is equal to 5.7 as shown in Figure 4.13.

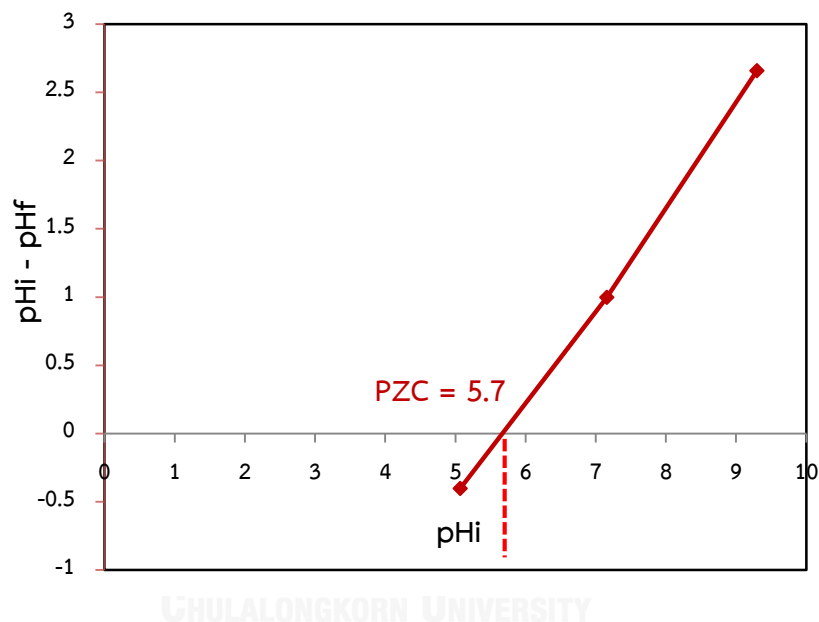


**Figure 4.13** The PZC of amorphous alumina measured by using titration method.

From the result of PZC of amorphous alumina, it can be concluded that when pH of solution is lower than 5.7 (e.g., pH 4), the specimen surface is filled with  $\text{H}^+$  ion and the surface defect is not found. On the other hand, when pH of solution is higher than 5.7 (e.g., pH 9), the surface charges on the specimen will be replaced with  $\text{OH}^-$  ions. These  $\text{OH}^-$  ions participate in the defect formation, leading to the more defective on the surface. Therefore, it can be clearly seen that the result of PZC measurement corresponding to the study of the pH effect. For this reason, the

corrosion of the amorphous alumina can be used to confirm that it is indeed caused by the hydrolysis reaction between specimen surface and the hydroxyl group in water.

#### 4.3.3 The effect of oxygen content in water.

According to the previously researches, the primary causes of the corrosion are many substances, such as carbon dioxide, chloride, the dissolve oxygen, and bacteria [20]. Thus, this experiment is done on the assumption that whether or not the amount of oxygen content in DI water affects this system. The design of this experiment is discussed in section 3.2.2.3. In summary, both conditions (at the temperature 50°C and 60°C), are repeated several times. The results are shown in Figure 4.14 and 4.15.

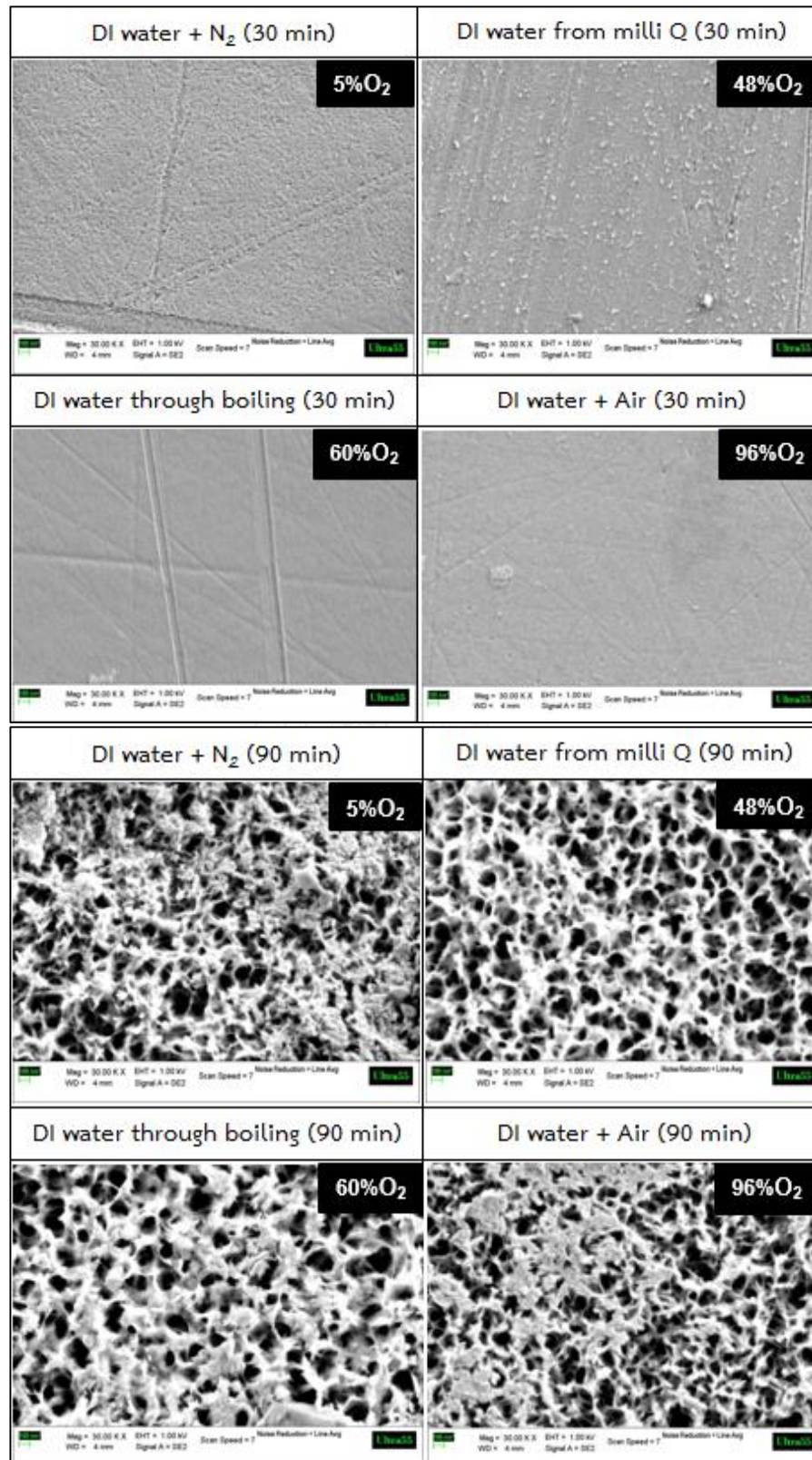


Figure 4.14 SEM micrograph of the specimen after immersed in DI water with various the amount of oxygen and immersion time at the temperature of 50°C.

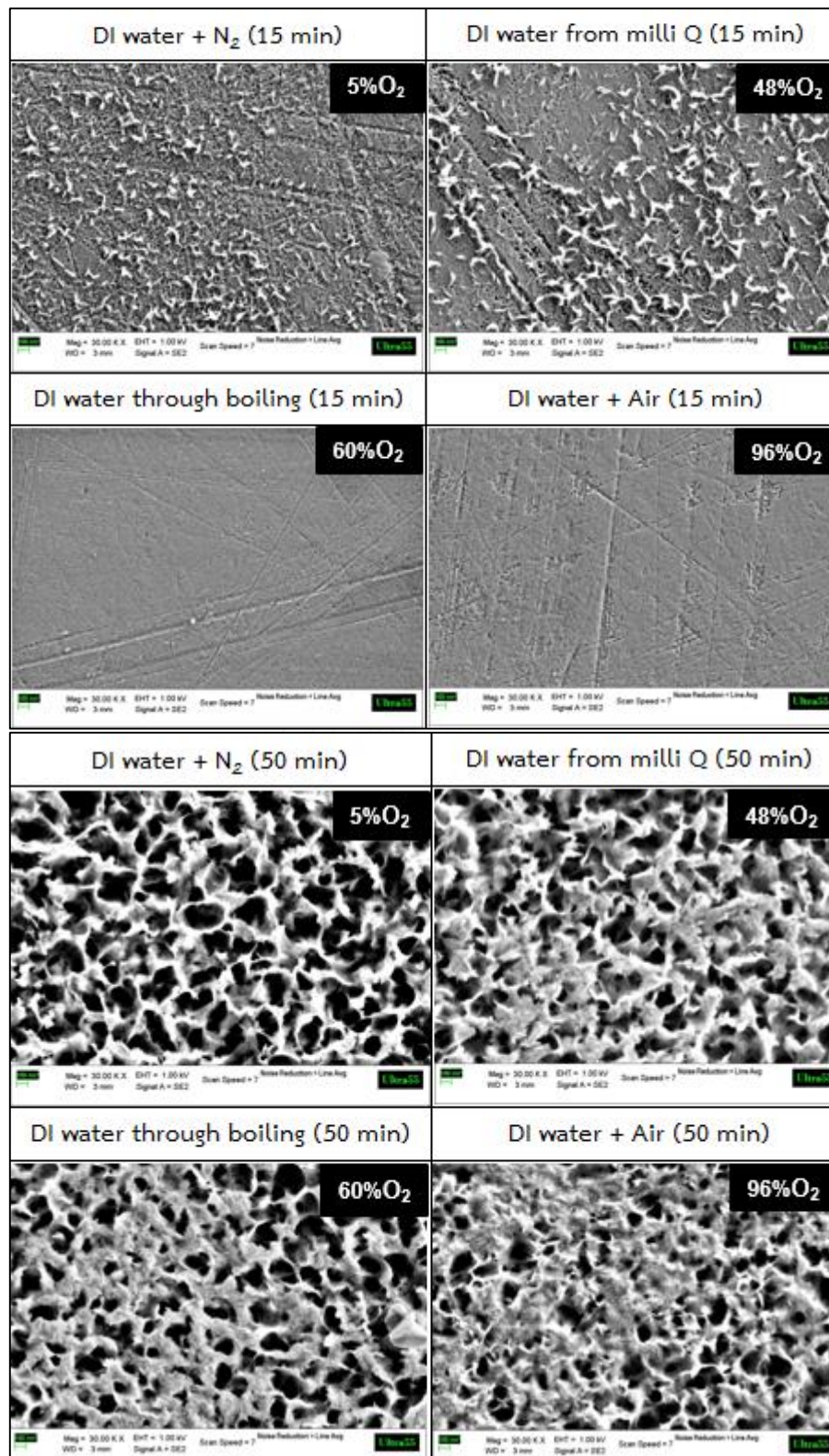
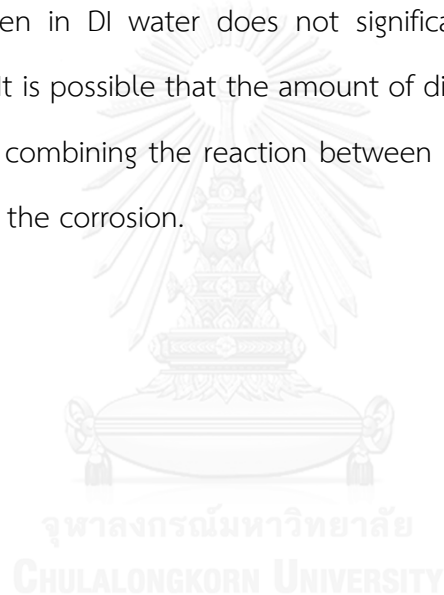


Figure 4.15 SEM micrograph of the specimen after immersed in DI water with various the amount of oxygen and immersion time at the temperature of 60°C.

From Figure 4.14 and 4.15, the results from both conditions tend to be similar. The specimen cannot be found the defect in condition that is not expected to see the defect (at 50°C for 30 min or at 60°C for 15 min). Although the defect is slightly found at 60°C, immersion time 15 minutes, but it is not severe level, thus it can be ignored. Likewise, the defect can absolutely be found on the surface specimens in conditions that could see the defect (at 50°C, immersion time 90 min and at 60°C, immersion time 50 min) even the water has different oxygen content. Therefore, the results from these experiments in this session can be concluded that the amount of oxygen in DI water does not significantly affect the corrosion of amorphous alumina. It is possible that the amount of dissolved oxygen in this system does not enough for combining the reaction between oxygen and liquid compound which cannot lead to the corrosion.



#### 4.3.4 The effect of ions content in water

According to the FTIR analysis of alumina-coated coupon, it is hypothesized that the hydroxyl ion ( $\text{OH}^-$ ) reacts with the alumina, resulting in observed defects. Different type of anions may differently interact with  $\text{Al}^{3+}$  in the alumina layer. In this session, the corrosion tests are done in order to investigate the influence of ions in DI water on the alumina surface. The synergistic effect is believed that to occur at the interface. Both of anions and cations are tested as following described.

##### 4.3.4.1 The effect of anion

For anions, there has a hypothesis that the surface of alumina is amorphous. The aluminium atoms contain lots of incomplete bonding. These atoms are very active and positively charged in nature. The addition of some anions may be reacted with the alumina instead of OH group and resulting in the formation of the new protective layer. Moreover, these anions may prevent the reaction between alumina and OH group, the further reaction or greater defect formation. The hypothesis model is shown in Figure 4.16.

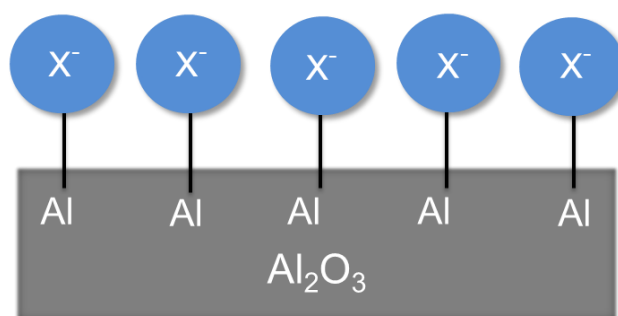


**Figure 4.16** The hypothesis of alumina surface model after added some anions in DI water.

The anions investigated in this study are chloride ion ( $\text{Cl}^-$ ), bromide ion ( $\text{Br}^-$ ), nitrate ion ( $\text{NO}_3^-$ ) and phosphate ion ( $\text{PO}_4^{3-}$ ), which are adjusted in different concentration and immersion time. The results are shown in Figure 4.17 - 4.20.

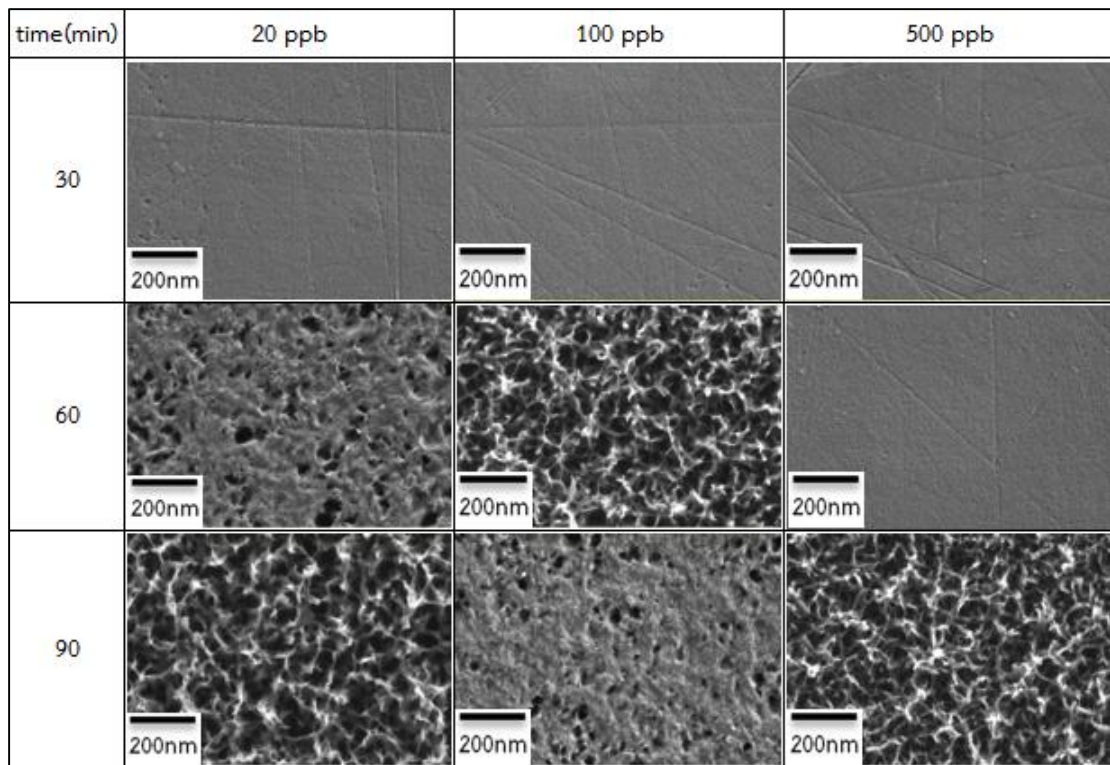


**Figure 4.17** SEM images of specimen after immersing into solution with  $\text{Cl}^-$  in various the concentrations and period of time.

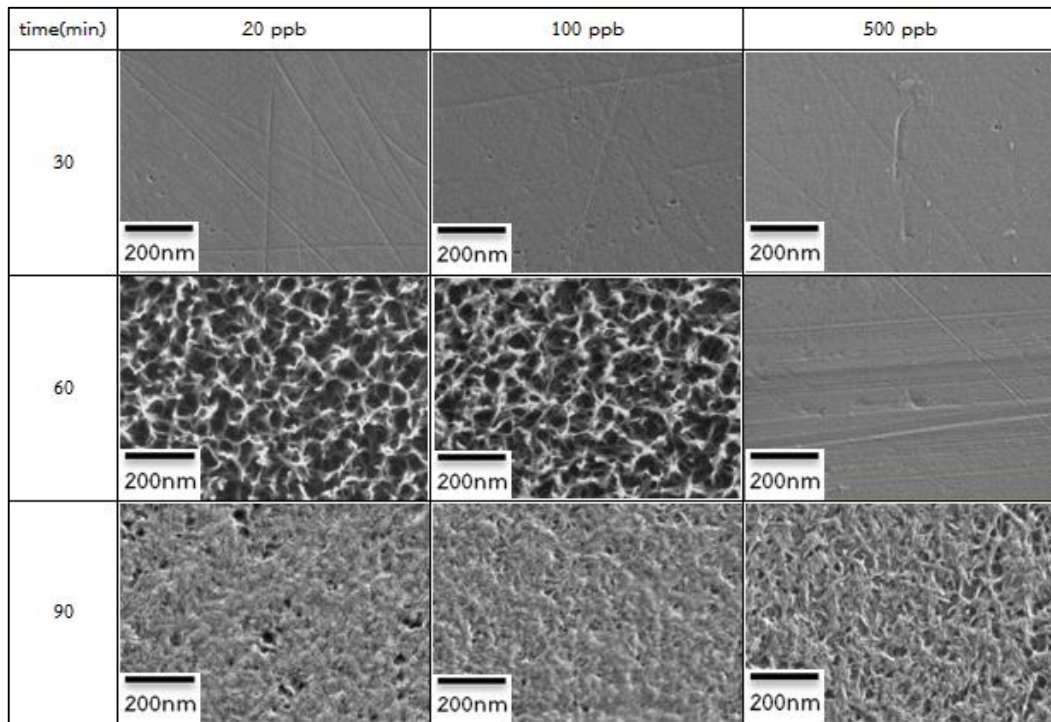


**Figure 4.18** SEM images of specimen after immersing into solution with  $\text{NO}_3^-$  in various the concentrations and period of time.

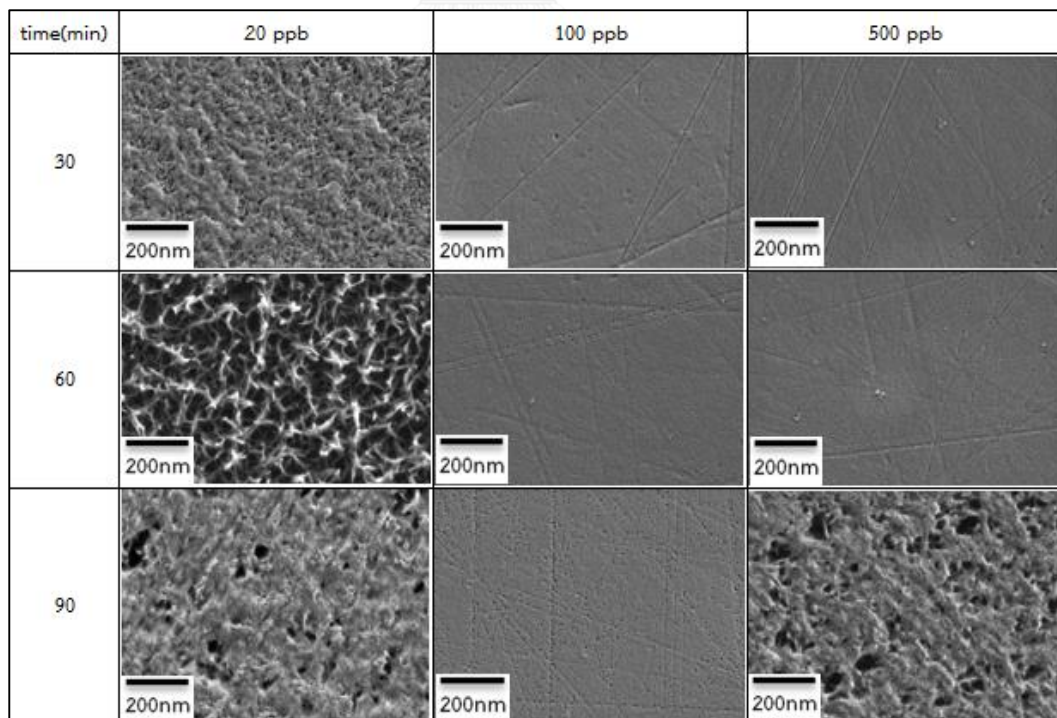


**Figure 4.19** SEM images of specimen after immersing into solution with  $\text{Br}^-$  in various the concentrations and period of time

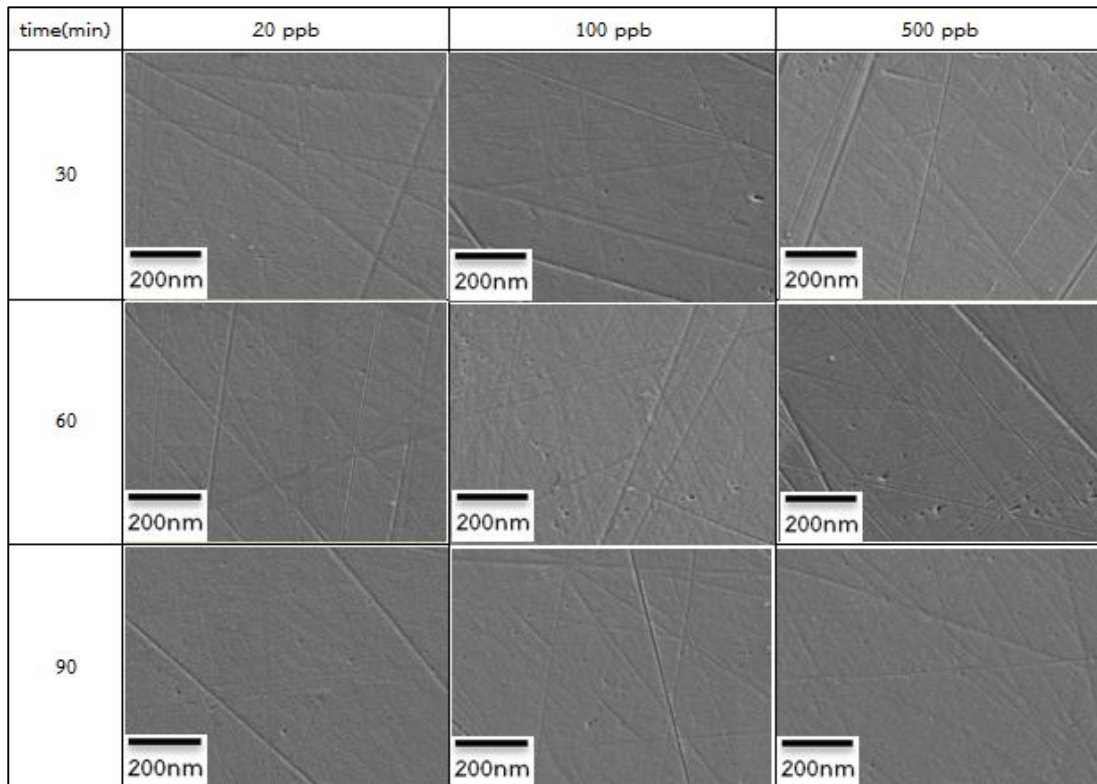


**Figure 4.20** SEM images of specimen after immersing into solution with  $\text{PO}_4^{3-}$  in various the concentrations and period of time.

The results from SEM images above, it can be written into information as shown in Table 4.3 for convenient explanation. The results represented in terms of either “YES” or “NO”. The definitions of “YES” or “NO” in each of the tables are described below:

- “NO” means the defect is not clearly observed on the specimen surface. This criterion is based on the average particle size which less than 106.24 nanometers as mentioned in session 4.2 (Table 4.2).
- “YES” means the defect is formed on the specimen surface with the average particle size larger than 106.24 nanometers as mentioned on session 4.2 (Table 4.2).

**Table 4.3** The data from SEM images show the effects of anions on the defect formation.

Experimental condition		Defect formed on the surface by SEM		
Ion	Concentrations (ppb)	Analysis		
		30 min	60 min	90 min
Cl <sup>-</sup>	20	NO	YES	YES
	100	NO	YES	YES
	500	NO	NO	YES
Br <sup>-</sup>	20	YES	YES	YES
	100	NO	NO	NO
	500	NO	NO	YES
NO <sub>3</sub> <sup>-</sup>	20	NO	YES	YES
	100	NO	YES	YES
	500	NO	NO	YES
PO <sub>4</sub> <sup>3-</sup>	20	NO	NO	NO
	100	NO	NO	NO
	500	NO	NO	NO

From the result in Table 4.3, it can be noticed that most of the anions can inhibit the corrosion on the alumina surface. If using the high concentration of anions (such as 500 ppb of Cl<sup>-</sup>, Br<sup>-</sup> and NO<sub>3</sub><sup>-</sup> ions), the corrosion tends to be decreased. Interestingly, the only ions that obviously showed the inhibition of the corrosion are PO<sub>4</sub><sup>3-</sup> ions, which work well at every concentration even in a long period of time. Therefore, the reaction between the surface of amorphous alumina and the phosphate ions may give the advantage to the other applications in further.

The study of the reaction behavior between phosphate ions and the alumina is needed because it still has a question whether the observed effect is a result from phosphate ions or potassium ions ( $K^+$ ). Since the chemical compound ( $K_3PO_4$  solution) is used in this experiment, therefore the effect of potassium ions must also be investigated first in order to prove whether  $K^+$  ions have any effect on the defect formation. In this work, the solution of  $KNO_3$  is used in the corrosion test as well in order to confirm these results. The result of using  $KNO_3$  is shown in Figure 4.21.

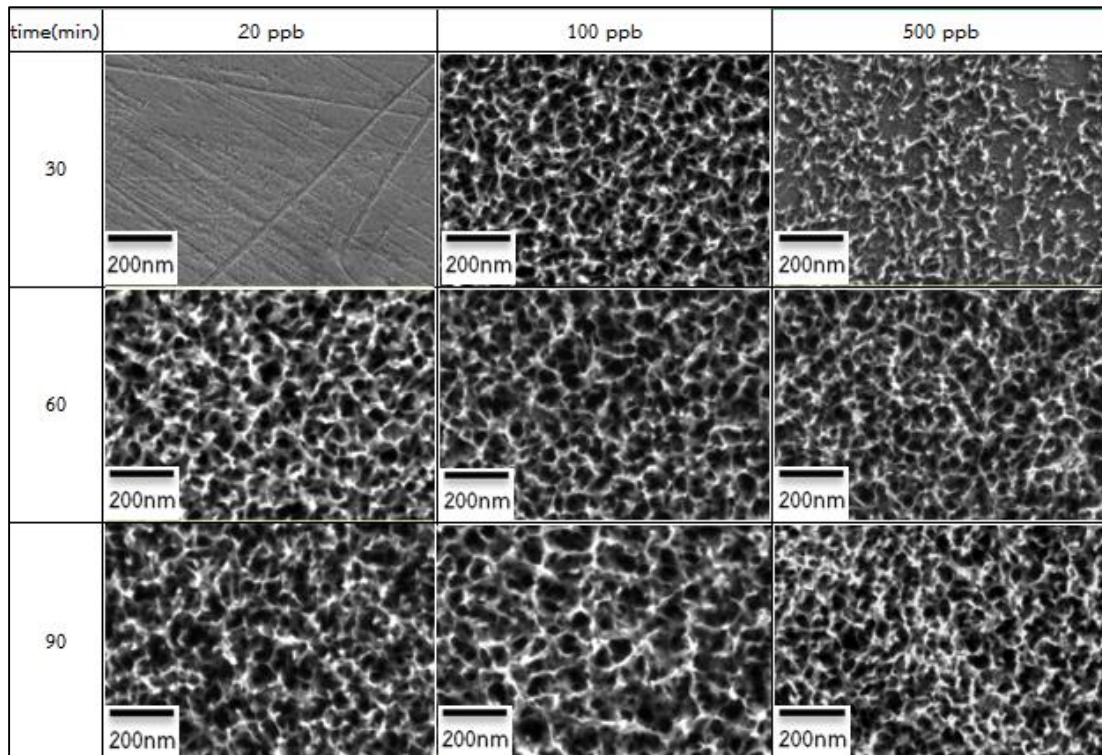
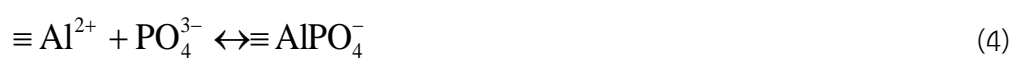
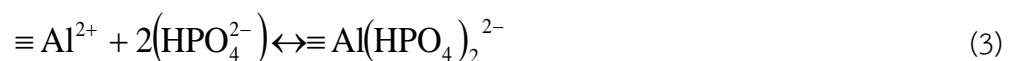


**Figure 4.21** SEM images of specimen after immersing into solution with  $K^+$  at the temperature of  $50^\circ C$  with various concentrations and period of time.

From the result in Figure 4.21, it indicated that  $K^+$  ions cannot prevent the defect formation on the specimen surface. Moreover, it seems likely that it accelerates the defect (as shown in SEM images at immersion time 30 minutes). The high concentration of  $K^+$  ions also enhances the defect. Therefore, all of these

investigations can be concluded that the phosphate ions in  $K_3PO_4$  solution are the only ions that prevent the defect on the alumina surface. It is possible that when the  $PO_4^{3-}$  ions reacted with water or reacted with the alumina surface, it will lead to the corrosion protection. Therefore, it is crucial to study this phenomenon deeply in details.

Generally, many researches have been studied about the adsorption of phosphate on the alumina. The pH of the solution is very an important parameter in this phenomenon. It is suggested that some ions are automatically released to the solution after mixing aqueous and phosphate solution. For examples,  $H^+$ ,  $Al(OH)^+_{2-}$ ,  $Al(OH)^{2+}$ ,  $Al^{3+}$ ,  $OH^-$ ,  $H_2PO_4^-$ ,  $HPO_4^{2-}$  and  $PO_4^{3-}$  are generated during the process of phosphate sorption. According to the system in which the alumina is exposed to DI water at pH 6.8, the addition of the  $K_3PO_4$  in the solution directly generate the ion species such as  $H^+$ ,  $OH^-$ ,  $PO_4^{3-}$  (excluding  $K^+$  ion) and  $Al(OH)^{2+}$  in which only presented at pH in the range of 4.5 to 7 [21]. Most of these ions are likely to undergo ligand exchange reaction by their electrostatic attraction on the surface. These reactions are shown in the following equations.



These reactions can take place at the interface area. It is the results from changing of the hydrogen bonding or changing of the surface hydroxyl group. Moreover, sorption mechanisms of phosphate have a tendency to increase rapidly at the initial state and occur simultaneously with the contribution of available sorption sites. This reaction is slow down when the reaction time is increased. Eventually, the combination reaction alumina between surface complexation and precipitation on the alumina interface is took place and it is directly related to the amount of hydroxyl in solution [22, 23]. Thus, it is clearly represented that  $\text{PO}_4^{3-}$  anions can be reacted with the alumina surface instead of  $\text{OH}^-$  group. These reactions resulted in the inhibition of the defect formation due to the decreased hydroxyl in sorption of phosphate process. The results correspond to the hypothesis as shown in Figure 4.16. However, this experiment cannot use to confirm the existing of  $\text{OH}^-$  group in the precipitate occurred on the specimens which had been analyzed by ATR-FTIR analysis because this method cannot detect the P-O stretching vibration. It is possible that the amount of phosphate which precipitated on the alumina surface is too small.

#### 4.3.4.1 The effect of cations

As for cations, the addition of some cations in DI water is done by following the hypothesis as shown in Figure 4.22. If the system is added with some cations, these ions should surround on the specimen surface and may form complex with water or hydroxyl ions instead of forming themselves on the alumina surface. The reduction in the number of  $\text{OH}^-$  groups resulted in the significantly decreased of the amount of the defect formation since these cations drawn the  $\text{OH}^-$  ions away from the specimen surface and cause no reaction on the specimens as well.

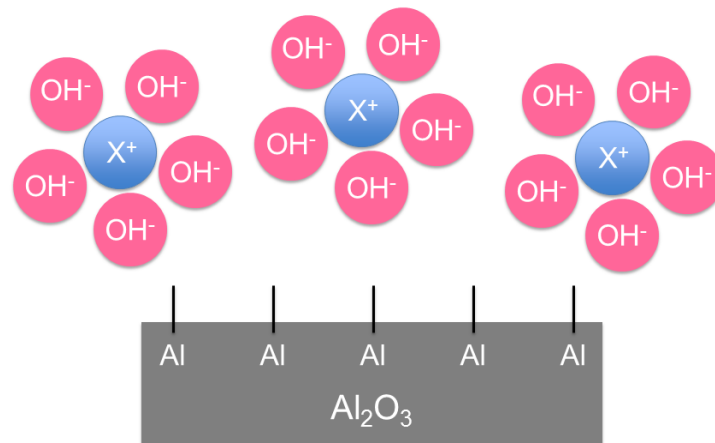


**Figure 4.22** The hypothesis of alumina surface model after added some cations in DI water.

The cations that are used in this experiment including  $Mg^{2+}$  ion (from  $Mg(NO_3)_2$ ),  $Zn^{2+}$  ion (from  $ZnSO_4$ ) and  $Al^{3+}$  ion (from  $Al(NO_3)_3$ ). These cations are used in different concentrations (20-500 ppb). The results are shown in Figure 4.23 to 4.25.

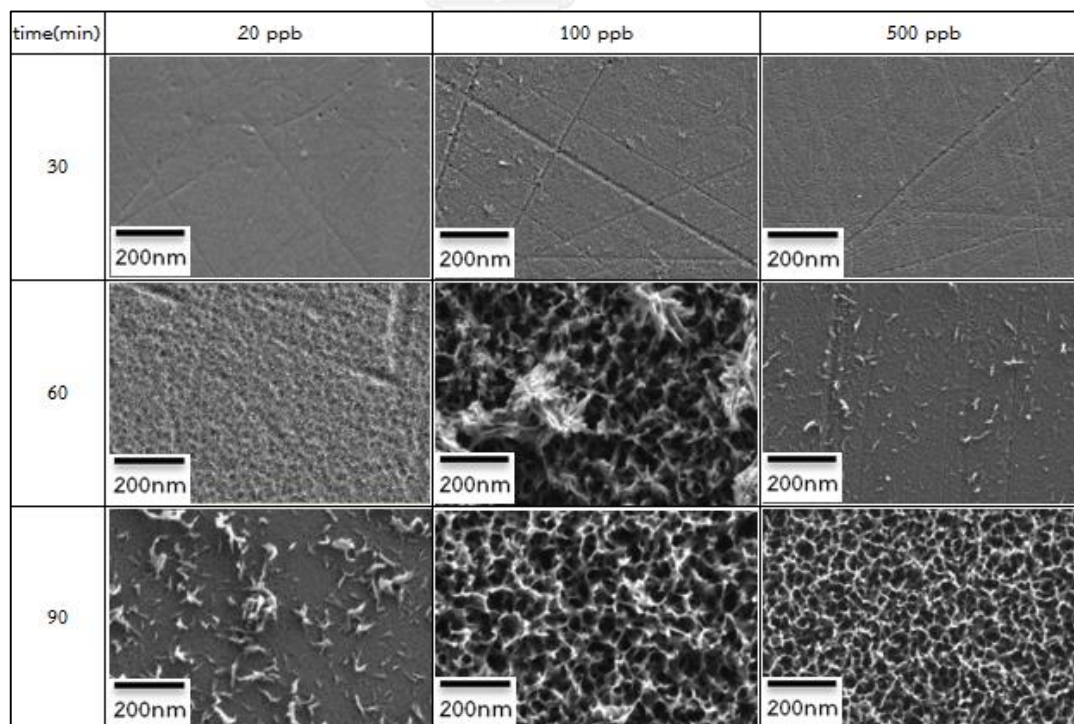


**Figure 4.23** SEM images of specimen after the specimen is immersed in solution mixed with  $Al^{3+}$  ion in various the concentrations and period of time.

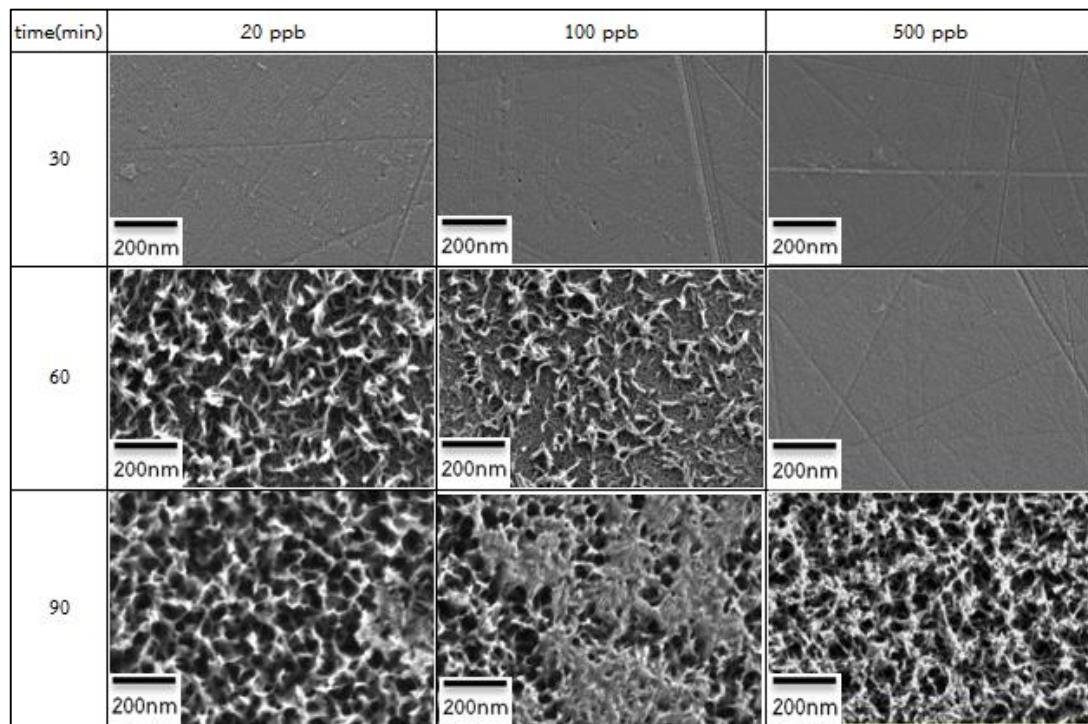


**Figure 4.24** SEM images of specimen after the specimen is immersed in solution mixed with  $Mg^{2+}$  ion in various the concentrations and period of time.

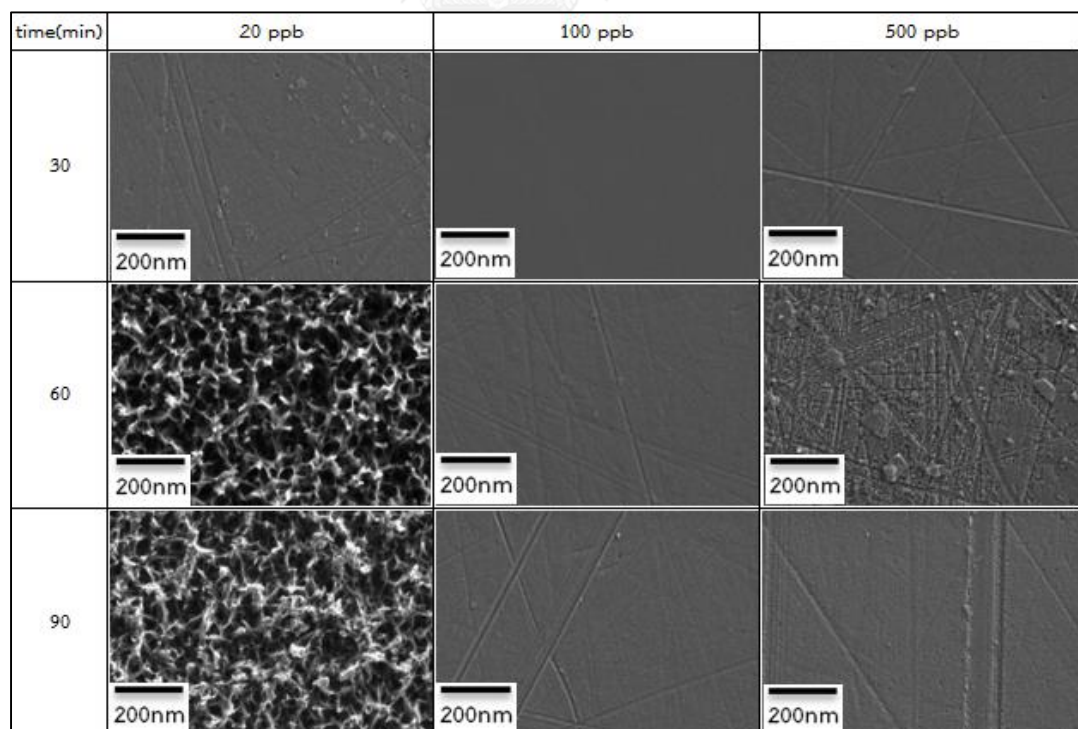


**Figure 4.25** SEM images of specimen after the specimen is immersed in solution mixed with  $Zn^{2+}$  ion in various the concentrations and period of time.

Similarly with anions, the SEM results of cations can be written into information as shown in Table 4.4 for convenient explanation.

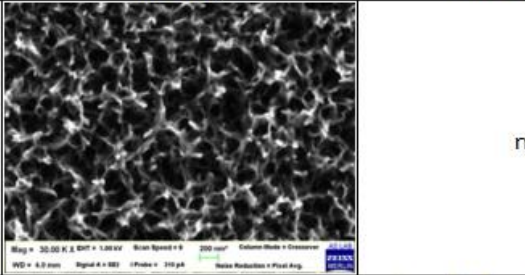
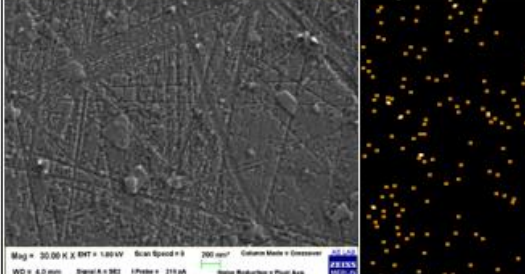
**Table 4.4** The effects of cations on the defect formation of the specimen.

Experimental condition		Corrosion formed on the surface by SEM		
Ion	Concentrations (ppb)	Analysis		
		30 min	60 min	90 min
Al <sup>3+</sup>	20	NO	YES	YES
	100	NO	YES	YES
	500	NO	NO	YES
Mg <sup>2+</sup>	20	NO	YES	YES
	100	NO	YES	YES
	500	NO	NO	YES
Zn <sup>2+</sup>	20	NO	YES	YES
	100	NO	NO	NO
	500	NO	NO	NO

The results from the addition of some cations in different concentrations indicated that both Al<sup>3+</sup> ions and Mg<sup>2+</sup> ions seem to have the behavior like the previous finding even no addition of any ions. Nothing is found in this experiment because the defect is still formed on the surface at the condition that expected the defect formation. On the contrary, the Zn<sup>2+</sup> ions concentrations that can inhibit the defect formation are at the concentration of 100 to 500 ppb. Since the defect formation was not found on the surface, it can be concluded that Zn<sup>2+</sup> ions form complex with water or OH<sup>-</sup> group at high concentration and it has a potential to prevent the defect. The reaction between Zn<sup>2+</sup> ions and OH<sup>-</sup> group in DI water can be described by adsorption phenomena [24] as shown in equation (5).



According to the Eqn.5, it can be used to explain about the surface complex formation which is formed between  $\text{Zn}^{2+}$  ions and aluminol groups through three processes; (I) surface complexation as mentioned in equation above, (II) dissolution process which is the dissolution between the alumina and the formation of  $\text{Zn}(\text{OH})_2$ . The increased hydroxide phase is a result from the increased alumina decomposition and (III) re-sorption process which is directly controlled by zinc loading in the solution. It is suggested that when the reaction time is increased, the formation of co-precipitated zinc-aluminum ( $\text{Zn}^{2+}$ - $\text{Al}^{3+}$  hydroxides) is found on the alumina surface [24]. In addition, this experiment could verify whether or not  $\text{Zn}^{2+}$  ions are precipitated on the alumina by using Time-of-flight secondary ion mass spectrometry (ToF-SIMS), which has high chemical sensitivity for detection of the elements and compositions on the specimen surface. The results are shown in Figure 4.26.

Sample	SEM Images	TOF-SIMS Images
Alumina with 20 ppb of $\text{Zn}^{2+}$		n/a
Alumina with 500 ppb of $\text{Zn}^{2+}$		

**Figure 4.26** The comparison between SEM images and ToF-SIMS analysis of the specimens after the specimen is immersed in DI water mixed with  $\text{Zn}^{2+}$  ions at various concentrations.

From the result in Figure 4.26, it revealed that at the low concentration of  $Zn^{2+}$  ion (20 ppb), the defect is observed on the specimen surface. However, the zinc particle from the precipitate on the alumina surface cannot be identified by using ToF-SIMS. In contrast, it revealed that the high concentration of  $Zn^{2+}$  ions (500 ppb) could prevent the defect. This result refers to the SEM image. The presence of zinc on the surface is confirmed by using ToF-SIMS. The result can be concluded that the presence of zinc on the surface could be due to the abundant of zinc particles dispersed on the alumina surface. These results correspond to the hypothesis as mentioned previously. Thus, it seems to ensure that the addition of  $Zn^{2+}$  ions at the concentration that high enough can lead to the complex formation with the hydroxyl group. This phenomenon brings about the reduction of active surface on the alumina. Consequently, the amount of hydroxyl group that reacted with the alumina is diminished. No defect formed on the surface. Thus, it is the good alternative method for prevention of the defect formation on the alumina surface.

### 4.3.5 The effect of electron transfer on the specimen

This experiment is one of the several ways to confirm the effect of  $\text{OH}^-$  group in terms of the defect formation on the specimen. Generally, it is well recognized that the electron transfer between two metal surfaces can be possible to take place[25]. This system is driven by using DC power supply which is connected to the two specimens as previously mentioned. This power supply is used for induction of the electron transfer. At the positive electrode, the negative ions are attracted to this side and lost electrons (oxidation reaction) while the negative electrode can attract protons and gain electrons (reduction reaction). Therefore, it is hypothesized that the positive charge was surrounded with  $\text{OH}^-$  group which originated from decomposition of water. The rest of ions such as  $\text{H}^+$  ions are getting closer to the negative electrode as shown in Figure 4.27.

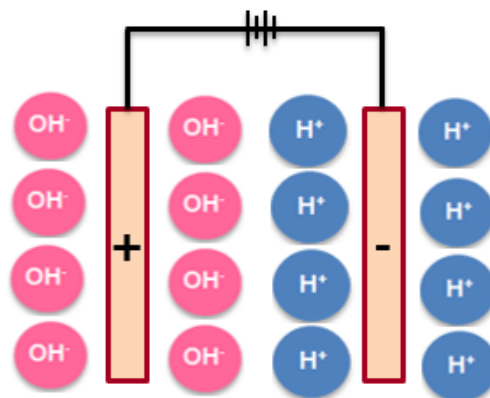


**Figure 4.27** Hypothesis of the specimens when applied potential to the system.

According to the hypothesis in Figure 4.27, if the  $\text{OH}^-$  group is the major cause of the defect, the defect formation of the specimen that connected to the positive electrode will be more severe than that connect to the negative electrode. The results are shown in Figure 4.28 to 4.30.

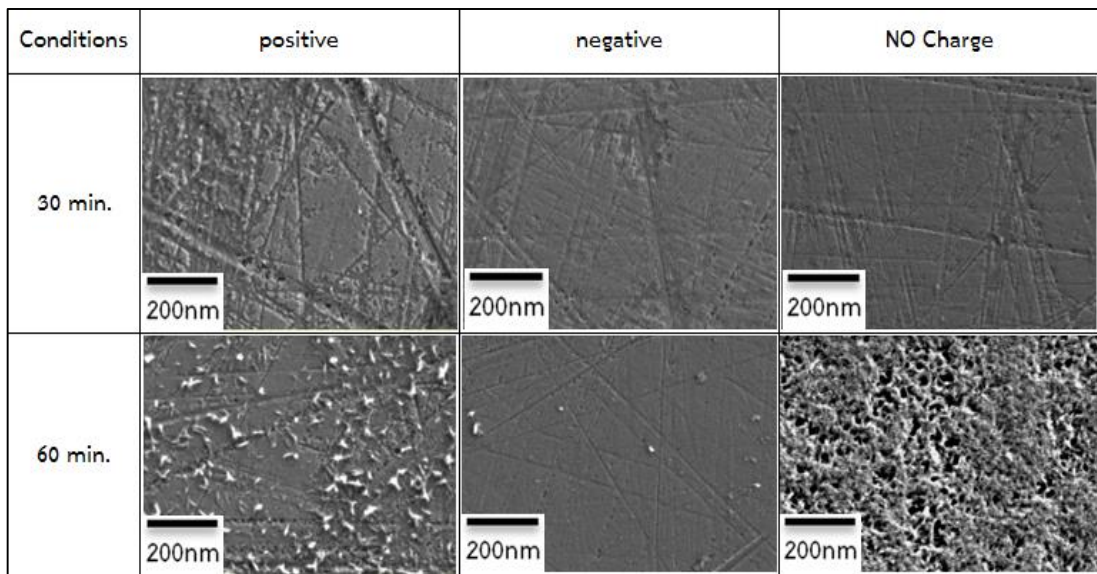


**Figure 4.28** The surface morphology of the alumina at each site of the electrodes after the specimen is immersed in DI water at 50°C with various period of time. The electric potential is applied at 6 V.

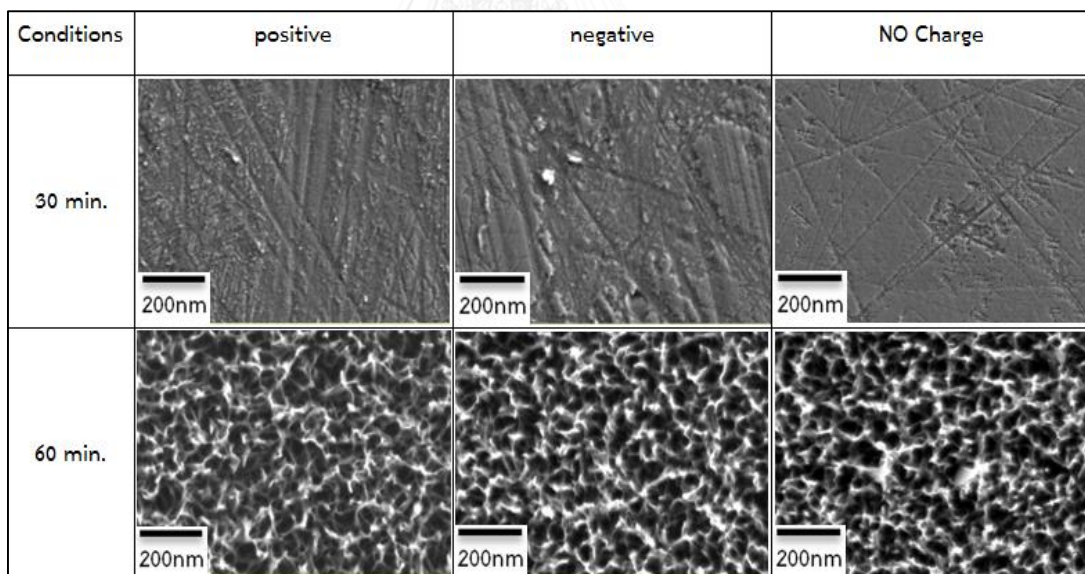


**Figure 4.29** The surface morphology of the alumina at each site of the electrodes after the specimen is immersed in DI water at 50°C with various period of time. The electric potential is applied at 15 V.

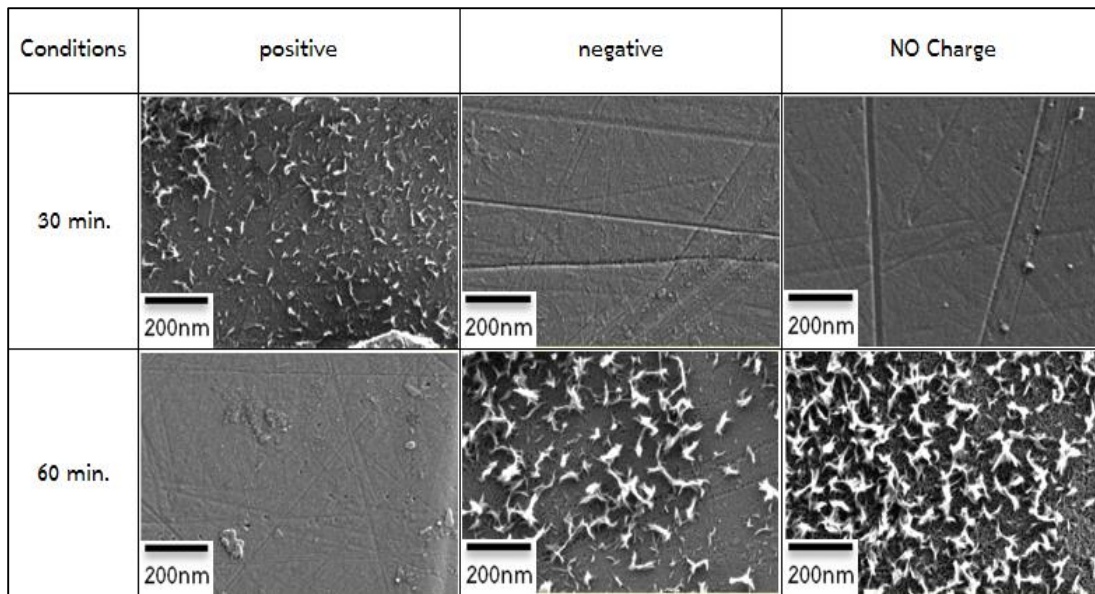


**Figure 4.30** The surface morphology of the alumina at each site of the electrodes after the specimen is immersed in DI water at 50°C with various period of time. The electric potential is applied at 20 V.

According to the SEM images results, the small defect formation is begun at the positive electrode after the electric potential is applied to the system at 6 volts (the lowest voltage in this experiment). It is consistent with the hypothesis which is mentioned above. Interestingly, the defect formation at the severe level can be detected at both of the electrodes after the electric potential is applied to the system at 15 volts. However, when the electric potential was increased up to 20 volts, the defect is only found at the negative electrode. Theoretically, the OH<sup>-</sup> ions or proton from the water dissociation tend to escalate at higher electric potential [26]. Thus, the more defect formation is expected after the voltage had supplied in this system. The results from some parts at this stage did not confirm the existing hypothesis and they cannot be explained the corrosion behavior by using other principles. Therefore, the effect of electron transfer at, the temperature of 60°C is used. The results are shown in Figure 4.31 to 4.33.

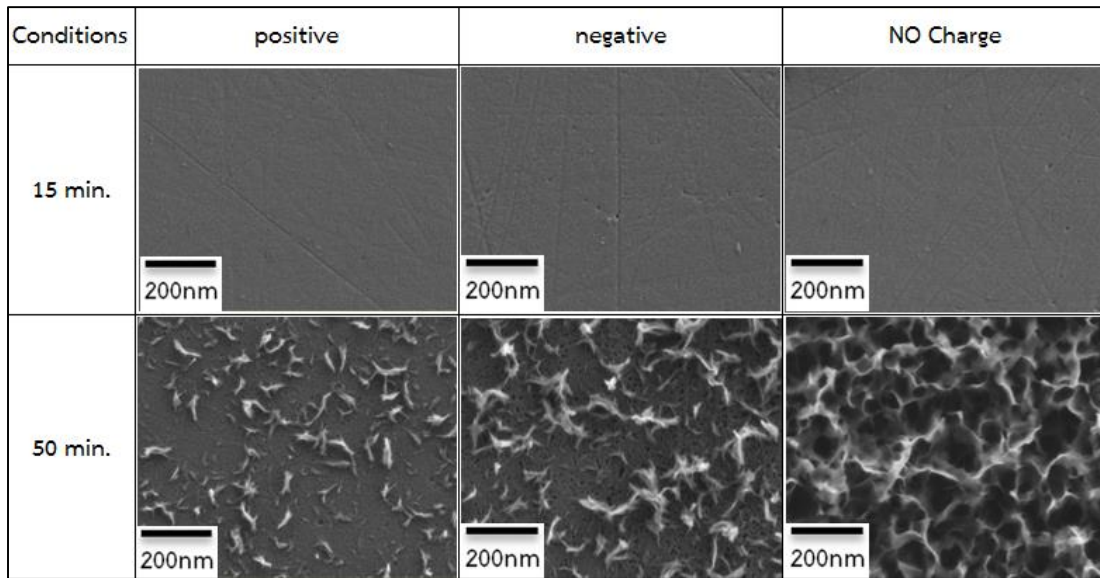


**Figure 4.31** The surface morphology of the alumina at each site of the electrodes after the specimen is immersed in DI water at 50 °C with various period of time. The electric potential is applied at 12 V.

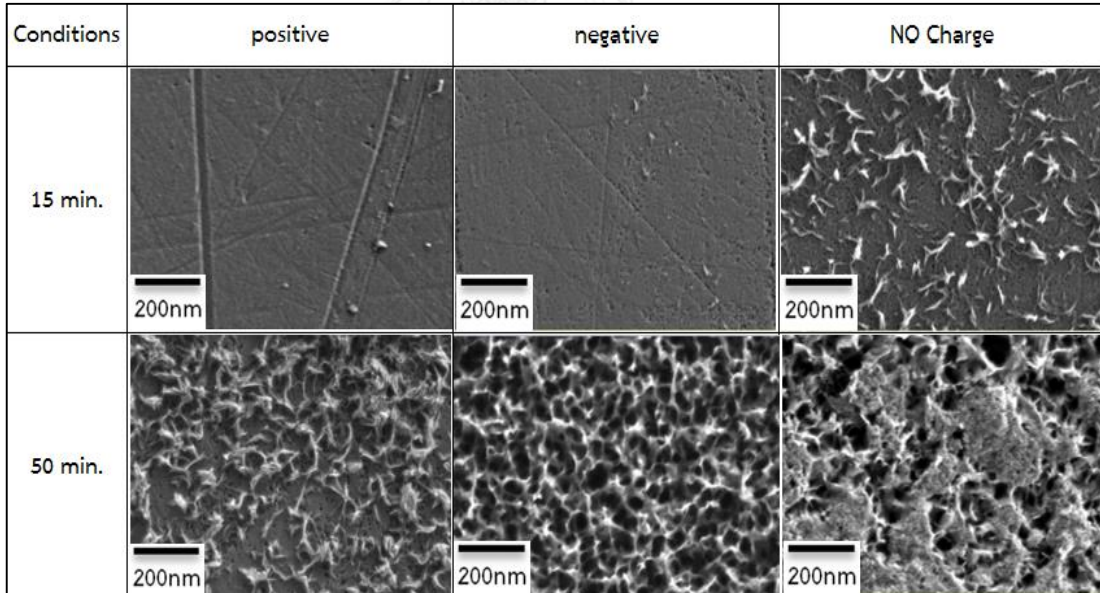


**Figure 4.32** The surface morphology of the alumina at each site of the electrodes after the specimen is immersed in DI water at 50 °C with various period of time. The electric potential is applied at 15 V.

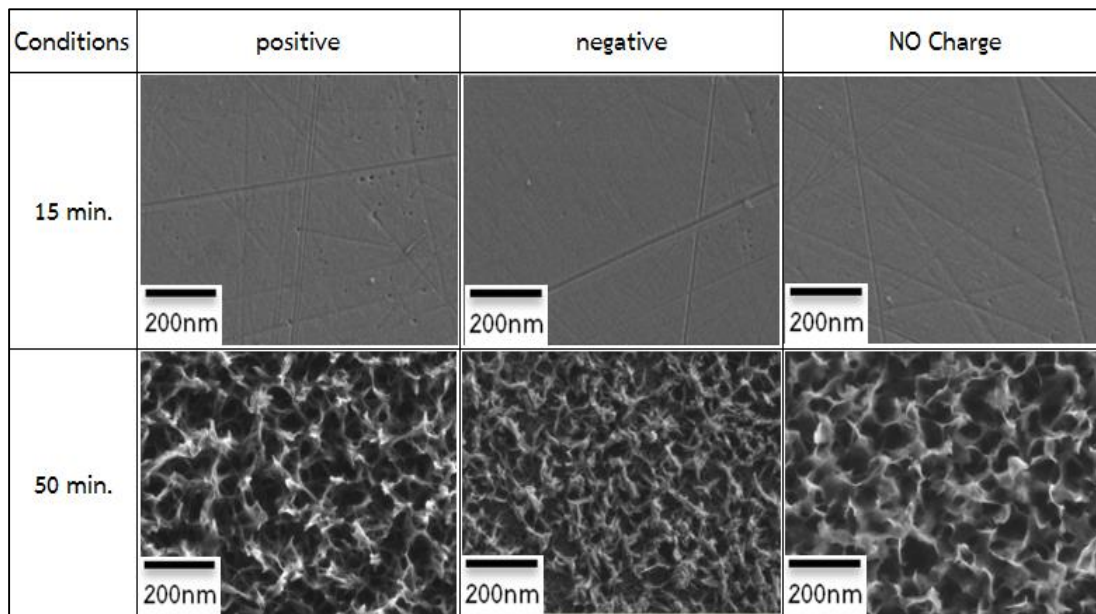


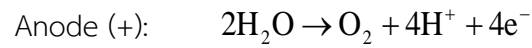
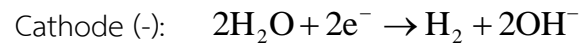
**Figure 4.33** The surface morphology of the alumina at each site of the electrodes after the specimen is immersed in DI water at 50 °C with various period of time. The electric potential is applied at 20 V.

The results at the temperature of 60°C, it contradicts the first hypothesis because two specimens tend to be observed the defect formation. Especially, the defect of the specimen that is connected to the negative electrode appeared to be more severe than the specimen that is connected to the positive electrode after the electric potential had applied at 12 and 15 volts. When the potential was supplied up to 20 volts, both electrodes have similar trend which is the increasing of the defect formation. The specimens have a different level of the defect formation which are result from the operating condition and the property of alumina. The results indicated that the connection to the negative electrode at high electric potential conditions cannot use to inhibit the defect in this system. It is possible that the corrosion behaviors in this work not only associated with the electron transfer but also involved in other reactions. The intrinsic reaction is needed to be investigated and described

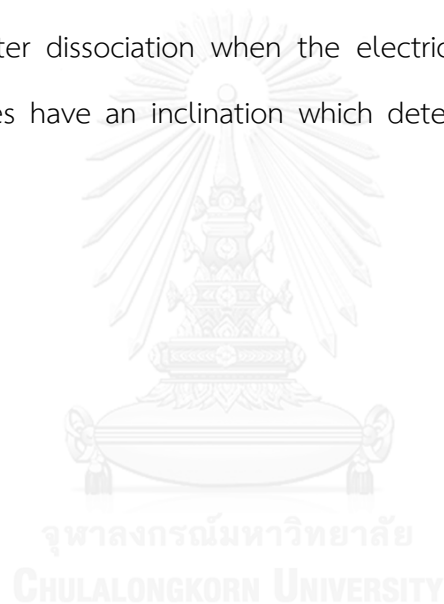
When applied the electric potential to the basic solution which already contained the two electrodes, the chemical system had transferred the reactant to another. This reaction is directly related to the redox reaction. The corrosion occurred to the atom or substance that lost the electron [27]. The ability to gain and donate the electron depends on the standard-state cell potential ( $E^\circ$ ) in each half-reactions. The overall cell potential ( $\Delta E^\circ$ ) must be the sum of the potentials between the oxidation and reduction half-reactions. If reactions for which  $\Delta E^\circ$  is positive, the reaction will give the favor for products forming and can be referred as the spontaneous reaction to take place. On the other hand, when the cell potential is negative, this means that the reaction would have to shift back toward the reactants to reach equilibrium and it needs to drive reactions with electric potential. For this experiment, it can be described by half-reactions for electrolysis of water process [28] as shown in the following equation.



The overall cell potential is also determined. The  $\Delta E^\circ$  is equal to  $-2.06\text{ V}$ , which means that this reaction will occur when the extra voltage at least  $-2.06\text{ volts}$  (overvoltage) is applied. Since this system is conducted in highly electric potential, it was easy to induce the electrolysis in the aqueous solution. According to the equations for the two half-reactions, each electrode can be classified as following:



According to the equations above, it is believed that the hydroxyl ion is the main cause of the defect. Thus, it can be easily observed at the negative electrode due to the more  $\text{OH}^-$  group generation. Although the positive electrode cannot generate the  $\text{OH}^-$  group, but it can absolutely attract the  $\text{OH}^-$  ion that increased rapidly from the water dissociation when the electric potential is enhanced [29]. Thus, both electrodes have an inclination which determined the defect formation simultaneously.

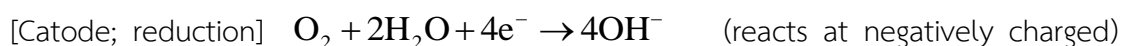


#### 4.3.6 The effect of dissolved oxygen coupled with the electron transfer

This factor is continuously considered from the previous part. The electron transfer also involved in the redox reaction because it transferred the reactant to another. This reaction can be done in basic solution. Considering the DI water system, the ions species that exist in nature includes  $H^+$ ,  $OH^-$ ,  $H_2O$ , and dissolved oxygen. Therefore, the half-cell reactions are possible to propose as following.



In this case, overall reaction are resulted from the equations (7) to (8), which are explained by the two redox reactions that have  $\Delta E^0$  equal to -1.63 V. The results indicated that the electric potential is required in order to drive this reaction at least 1.63 volts. The details of the electrolysis process are shown following:



In order to confirm these equations, the effect of the dissolved oxygen coupled with the electron transfer is studied. The corrosion test is repeated several times. The results are shown in Figure 4.34 to 4.37.

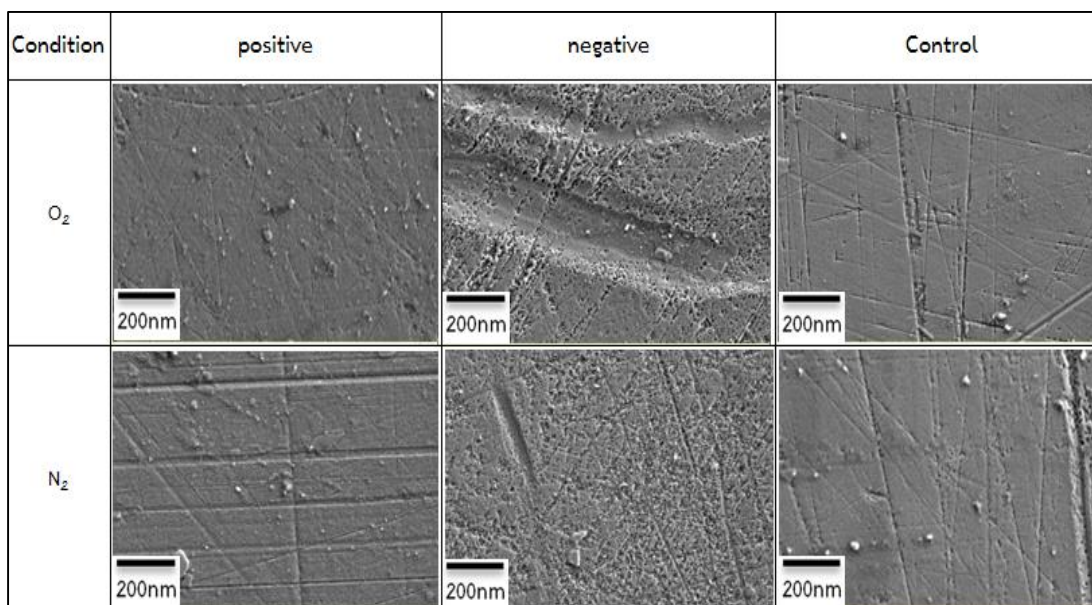


**Figure 4.34** The microstructure of the alumina surface when connected to each site of the electrodes and continuously bubbled O<sub>2</sub> and N<sub>2</sub> into DI water at 50° C for 30 minutes. The applied electric potential is 3 V.

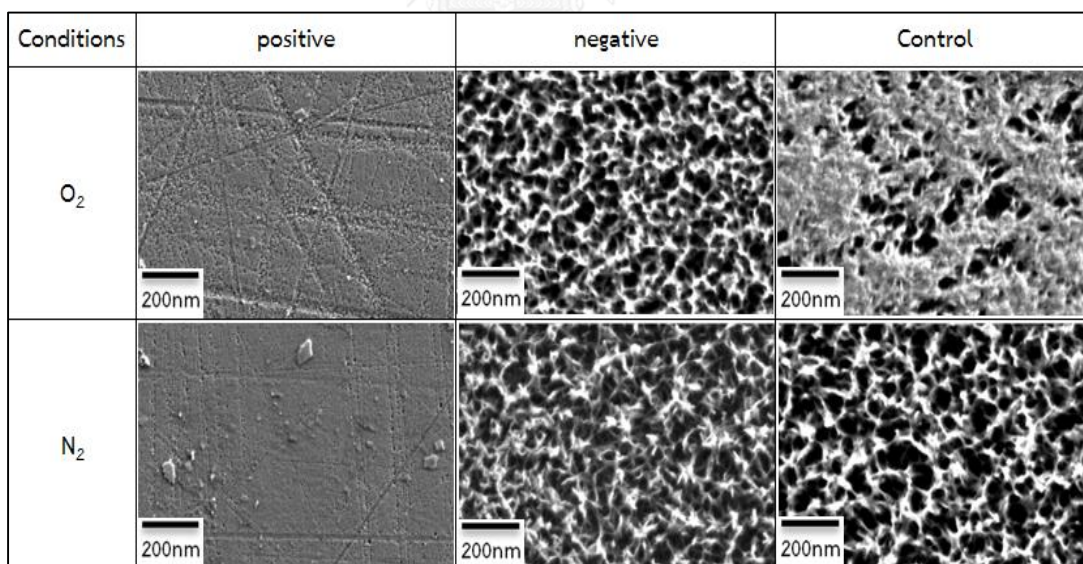


**Figure 4.35** The microstructure of the alumina surface when connected to each site of the electrodes and continuously bubbled O<sub>2</sub> and N<sub>2</sub> into DI water at 50° C for 60 minutes. The applied electric potential is 3 V.

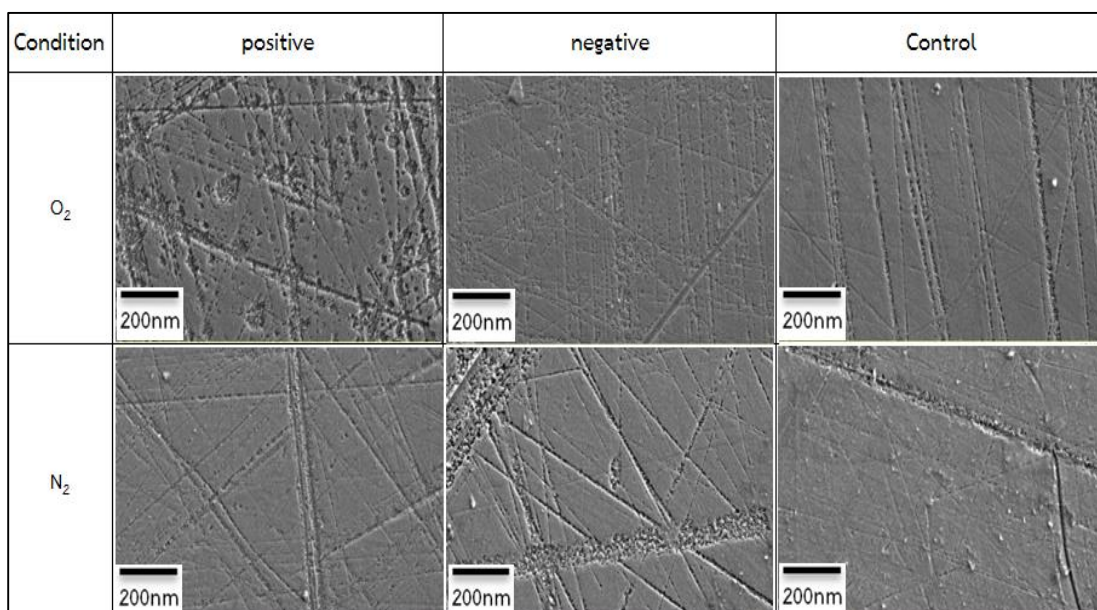


**Figure 4.36** The microstructure of the alumina surface when connected to each site of the electrodes and continuously bubbled O<sub>2</sub> and N<sub>2</sub> into DI water at 50° C for 30 minutes. The applied electric potential is 6 V.

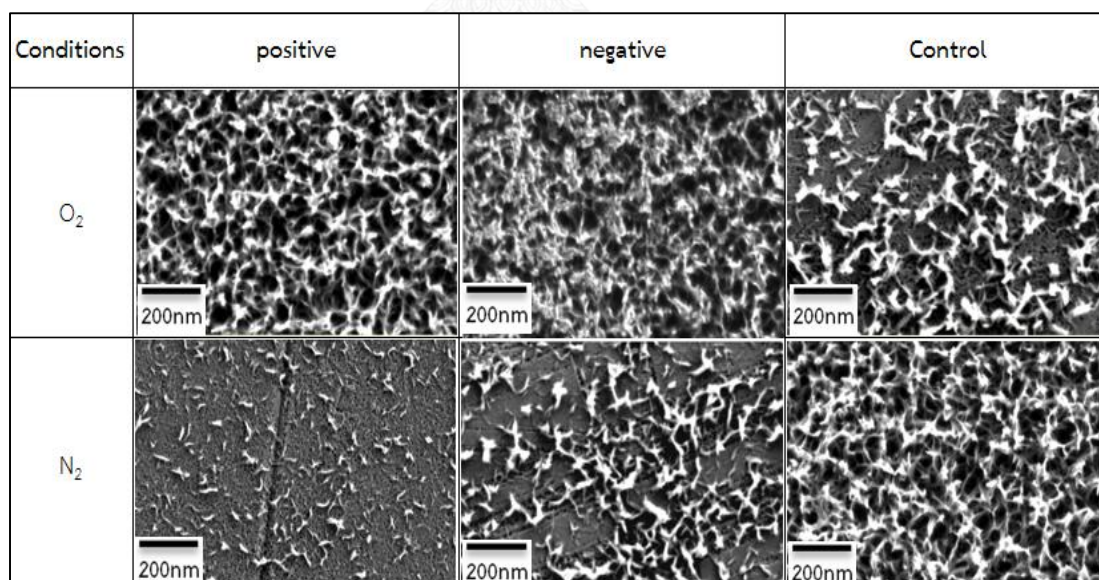


**Figure 4.37** The microstructure of the alumina surface when connected to each site of the electrodes and continuously bubbled O<sub>2</sub> and N<sub>2</sub> into DI water at 50° C for 60 minutes. The applied electric potential is 6 V.

According to the immersion time for 30 minutes, the specimens from both of the conditions that applied the electric potential at 3 volts and 6 volts did not change. The corrosion behavior is the same as the control specimen. The defect is not found in these conditions. On the other hand, when the immersion time is increased to 60 minutes, many effects which occurred on the specimens can be detected. Considering the negatively charged cathode, the reaction between dissolved  $O_2$  and  $H_2O$  ions takes place. The four electrons ( $4e^-$ ) are generated as many  $OH^-$  ions. In contrast, at the positively charged anode, an oxidation reaction occurs. There has a  $H_2O$  consumption which generated the oxygen gas, protons and gives electrons. Consequently, the defect formation had a higher chance for observation at the negative electrode. Especially, when the amount of dissolved oxygen is increased, the reaction shifts forward to higher  $OH^-$  production. Whenever the dissolved oxygen is diminished by purging  $N_2$  gas, the reaction at cathode will be reversed and the defect may also be decreased.

All reaction mechanisms at both sites of the electrodes which had mentioned previously correspond to the principle of the redox reaction. However, only one condition that is in exception. According to the positive electrode which had applied the voltage for 6 volts, 60 minutes and had increased the dissolved oxygen, the defect is formed on the surface. However, this phenomenon cannot be described why the defect is formed on the surface even it is connected to the positive electrode. Although this experimental condition is repeated many times, it is usually gives the results as shown in Figure 4.37. Nonetheless, the defect found on the specimen may be originated from the interaction of other factors. The corrosion behavior cannot be explained in these conditions.

### 4.3.7 The effect of local $H^+/OH^-$ concentration

This experiment is conducted the same as the session 4.3.5, but the specimens are not directly connected to the DC power supply. The specimens are immersed in DI water with differ in distance between the two electrodes. The hypothesis of this experiment is shown in Figure 4.38.

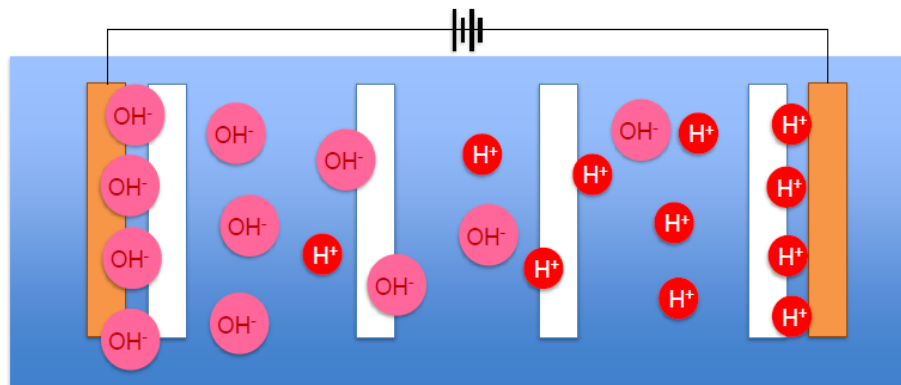


**Figure 4.38** The hypothesis for studying the effect of  $OH^-/H^+$  concentration.

It is believed that the  $OH^-$  group is the main cause of the defect. If the specimens are placed at the close position to the positive electrode, the defect formation will have more chance to occur because of the overwhelming coverage by the  $OH^-$  group. On the contrary, the defect formation which is occurred near the negative electrode may not be observed because this area has the lower concentration of  $OH^-$  group (it was replaced by  $H^+$  ions). The definition is shown in SEM images as described below.

- “(+) 1” means the specimen is far away from the positive electrode 1 mm.
- “(+)10” means the specimen is far away from the positive electrode 10 mm.

- “(-) 1” means the specimen is far away from the negative electrode 1 mm.
- “(-) 10” means the specimen is far away from the negative electrode 10 mm.

All of the investigations are done at the temperature of 50°C for 30 and 60 minutes of immersion time with various electric potential. The results are shown in Figure 4.39 to 4.46.

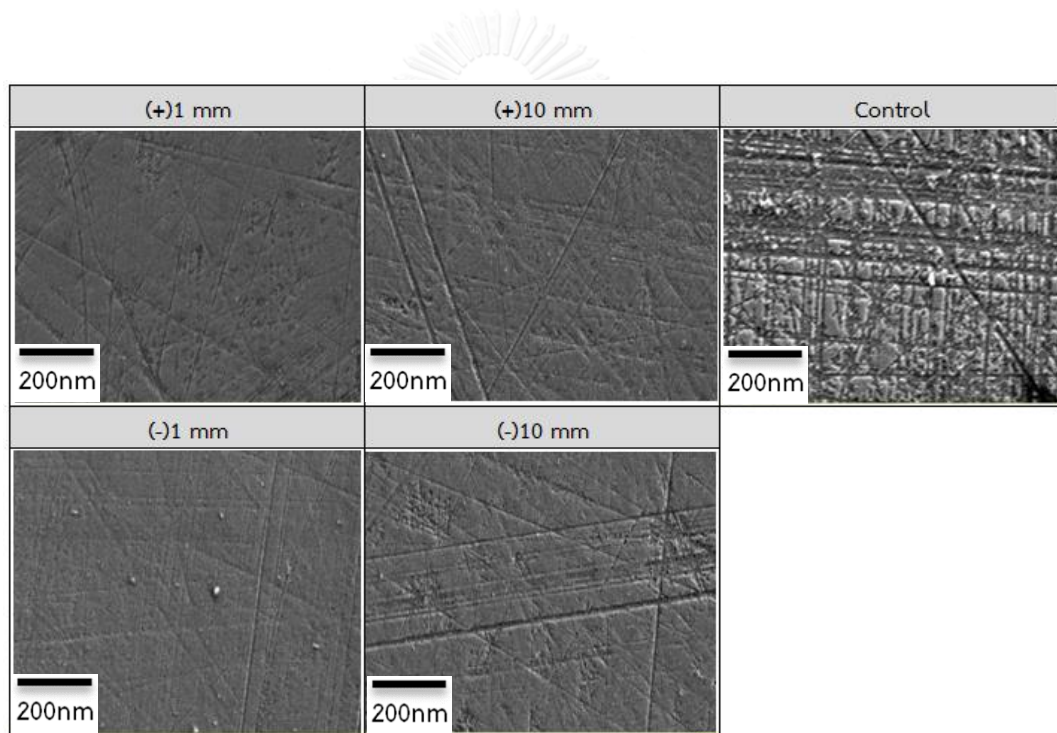


**Figure 4.39** The SEM images of the alumina layer after the specimens are immersed in DI water between the two electrodes at the temperature of 50°C for 30 minutes and applied electric potential 3 V.

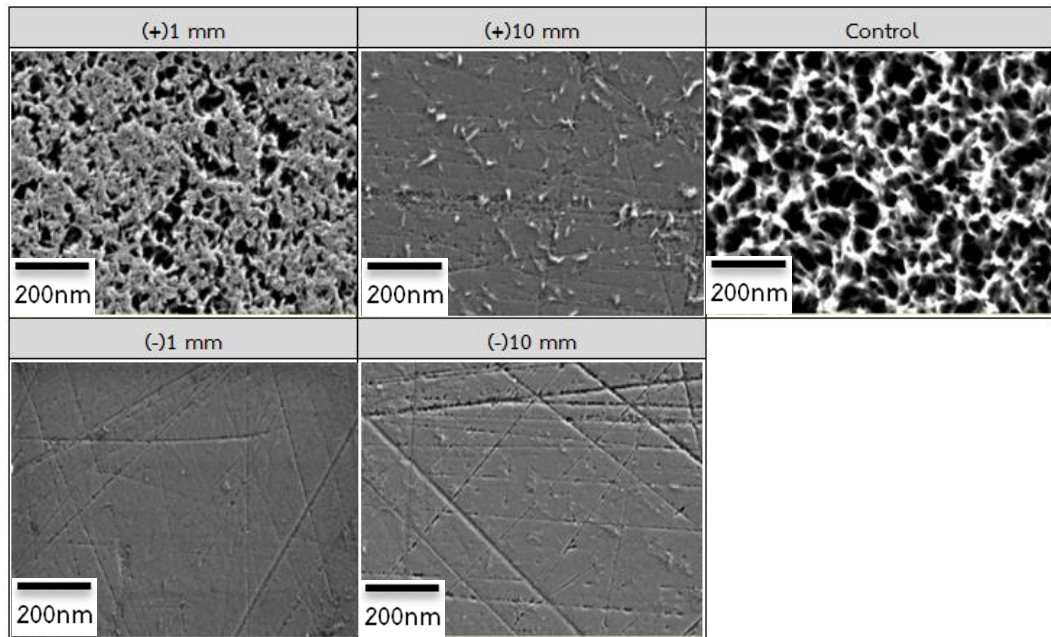


**Figure 4.40** The SEM images of the alumina layer after the specimens are immersed in DI water between the two electrodes at the temperature of 50°C for 60 minutes and applied electric potential 3 V.

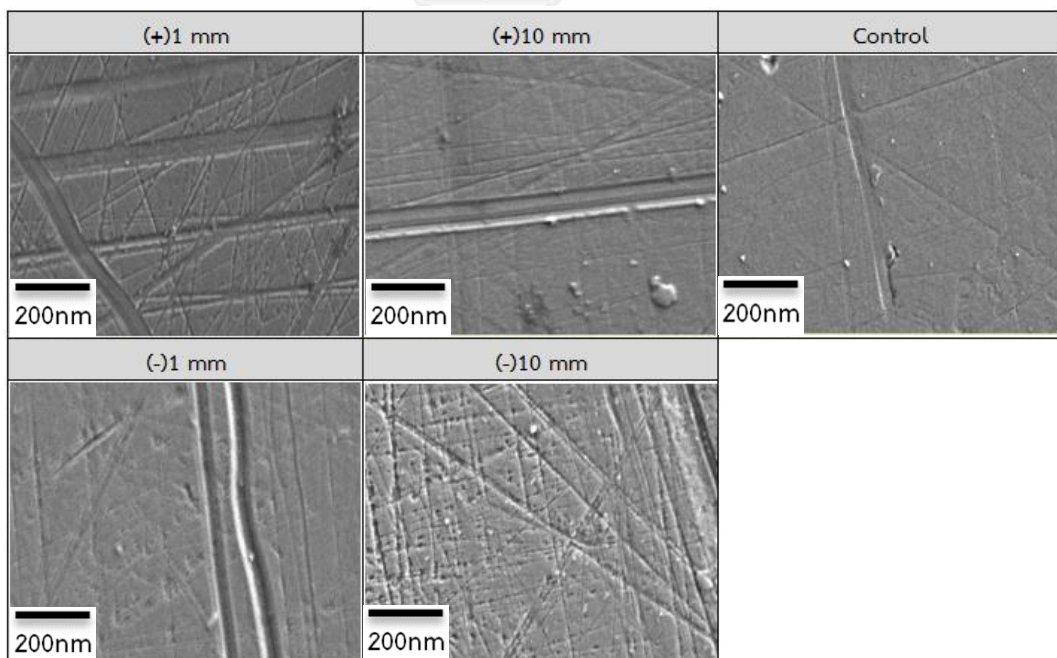


**Figure 4.41** The SEM images of the alumina layer after the specimens are immersed in DI water between the two electrodes at the temperature of 50°C for 30 minutes and applied electric potential 6 V.

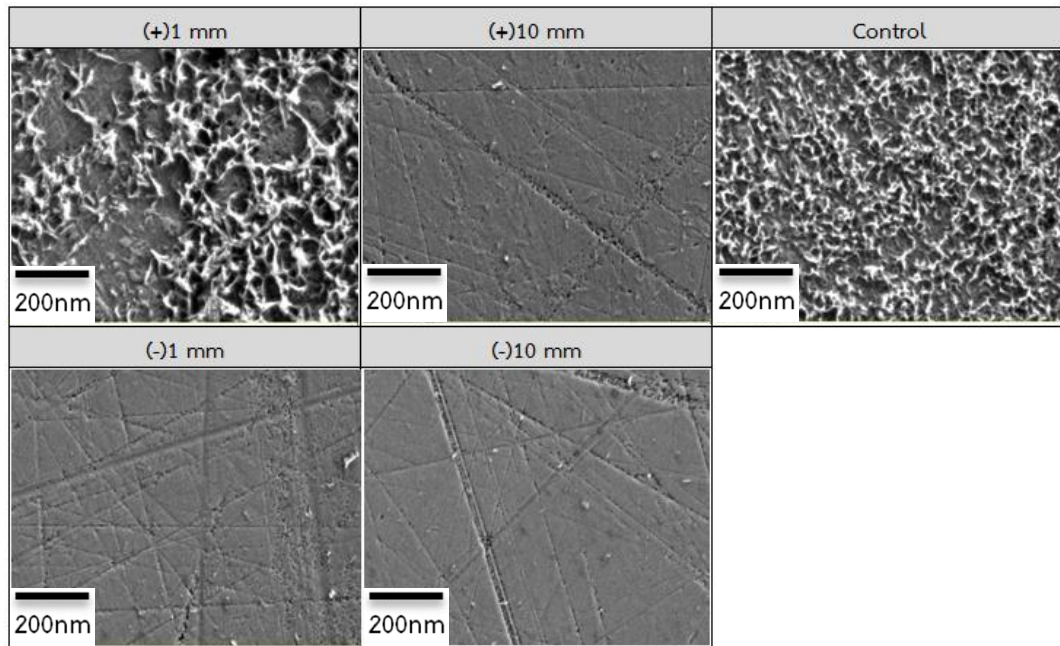


**Figure 4.42** The SEM images of the alumina layer after the specimens are immersed in DI water between the two electrodes at the temperature of 50°C for 60 minutes and applied electric potential 6 V.

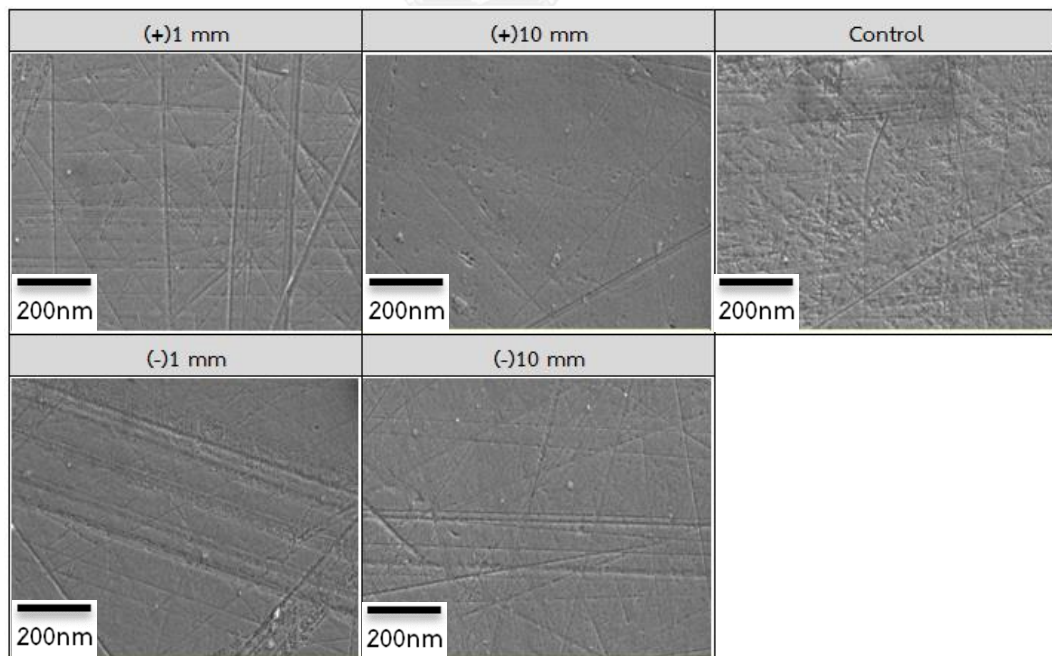


**Figure 4.43** The SEM images of the alumina layer after the specimens are immersed in DI water between the two electrodes at the temperature of 50°C for 30 minutes and applied electric potential 12 V.

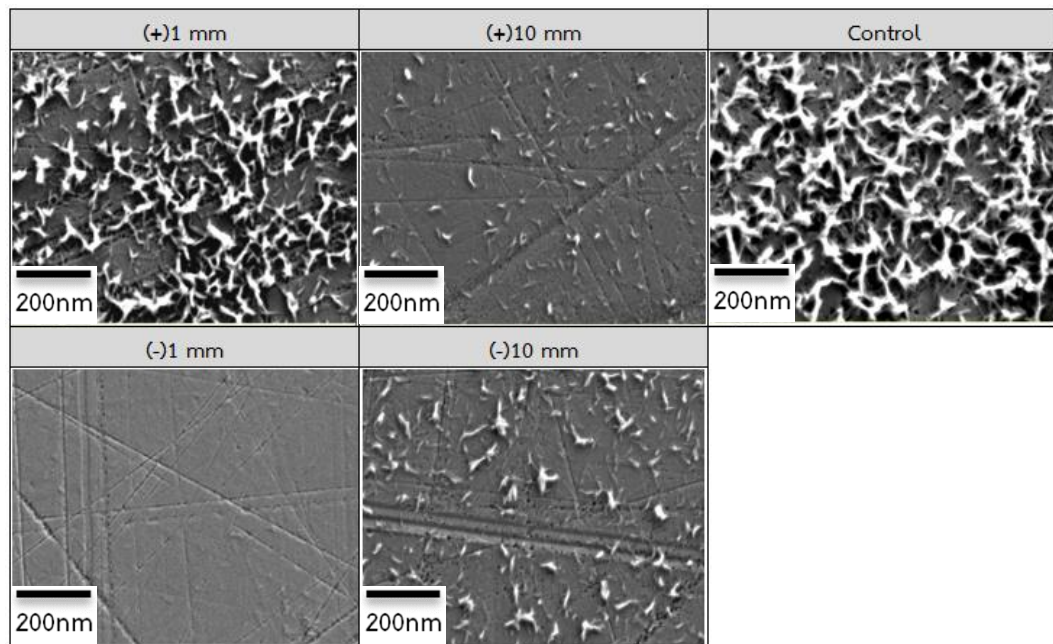


**Figure 4.44** The SEM images of the alumina layer after the specimens are immersed in DI water between the two electrodes at the temperature of 50°C for 60 minutes and applied electric potential 12 V.

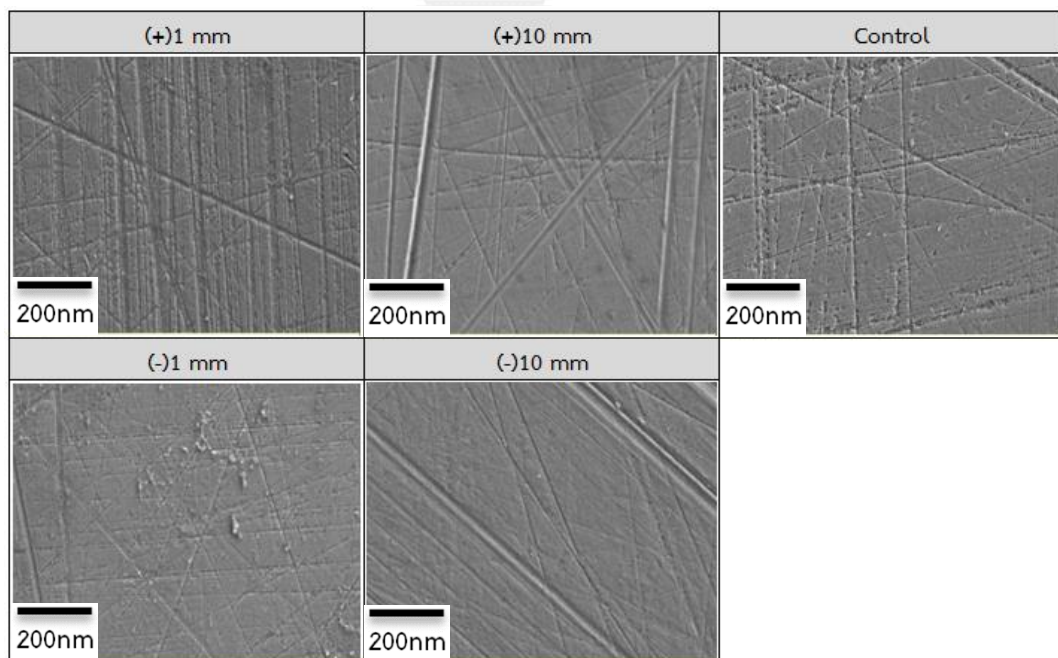


**Figure 4.45** The SEM images of the alumina layer after the specimens are immersed in DI water between the two electrodes at the temperature of 50°C for 30 minutes and applied electric potential 15 V.

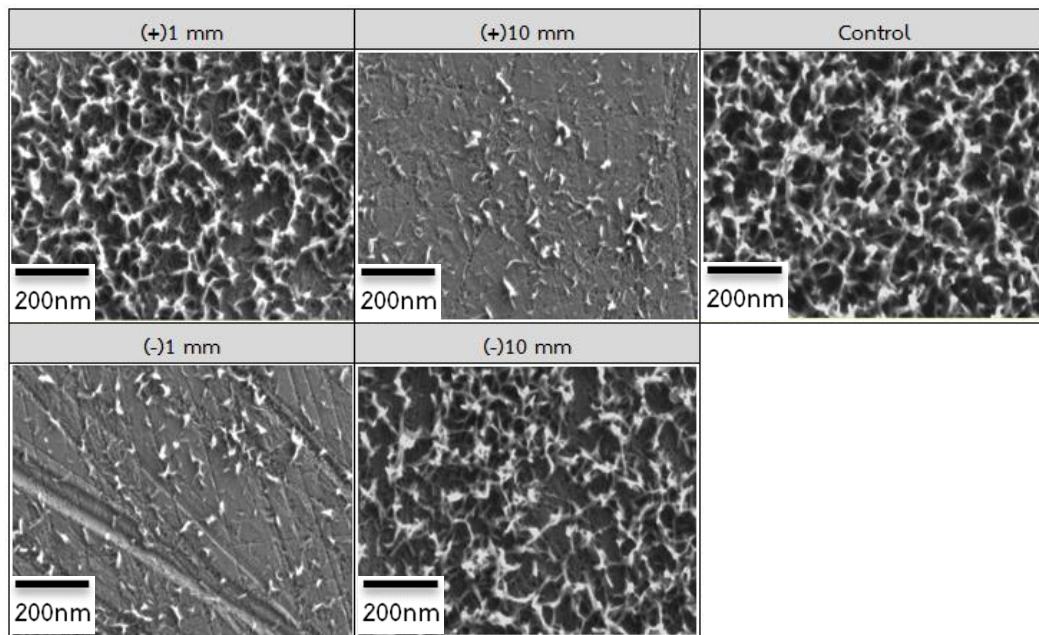


**Figure 4.46** The SEM images of the alumina layer after the specimens are immersed in DI water between the two electrodes at the temperature of 50°C for 60 minutes and applied electric potential 15 V.

From the experimental results, it is suggested that the defect formation did not observed on the alumina layer at the immersion time 30 minutes even the electrical is increased up to 15 volts. In contrast, when the immersion time is prolonged, the defect is gradually formed on the surface. This defect formation is depended upon the potential that is applied in the system. According to the electric potential at 3 and 6 volts, the defect is obviously formed on the specimen near the positive electrode while the defect is not found on the specimen near the negative electrode. Additionally, the specimen is placed far away from the electrode 1 mm seems to have more defect formation than the specimen which is placed far away from the electrode 10 mm. After the electric potential in the range of 12 to 15 volts had been applied to the specimen, the defect formation is begun appearing on negative electrode. Especially, after the electric potential at 15 volts, the defect

formation is hardly to distinguish between the two electrodes. From the results mentioned above, it can be explained by the dissociation of water in electron or proton transfer processes.

Most of researchers have been reported that the water molecules can be dissociated into  $H^+$  ions and hydroxyl ions. The increasing of these ion species depends on several factors such as the electrolyte solution, the electrode potential, and the electrode properties [30]. Thus, the concentration of  $OH^-$  species on the specimen that located between positive electrode and negative electrode is different. The surface defect that formed at the condition using the electric potential 15 volts is originated from the high generation of the  $OH^-$  species which are interacted with any ions in this extent, leading to the destruction of the alumina structure.

In another case, it can be explained by surface ionization reaction as well. Generally, the metal oxide surface, which is exposed in water, can generate the surface hydroxyl groups (Me-OH) that contribute to the fully hydroxylated surfaces. it is directly related to the counterion in the system. The changing of charge on the metal surface charge via surface ionization reaction is shown below.



Where  $K_{a1}$  and  $K_{a2}$  are the constant of surface ionization reactions. These constants depend on the material being used in the experiment. The Eq.10 and Eq.11 describe positively charged and negatively charged surface, respectively. The

atomic arrangements of the surface after the specimens were connected to both of the positive and negative charge on metal oxide are shown in Figure 4.47.

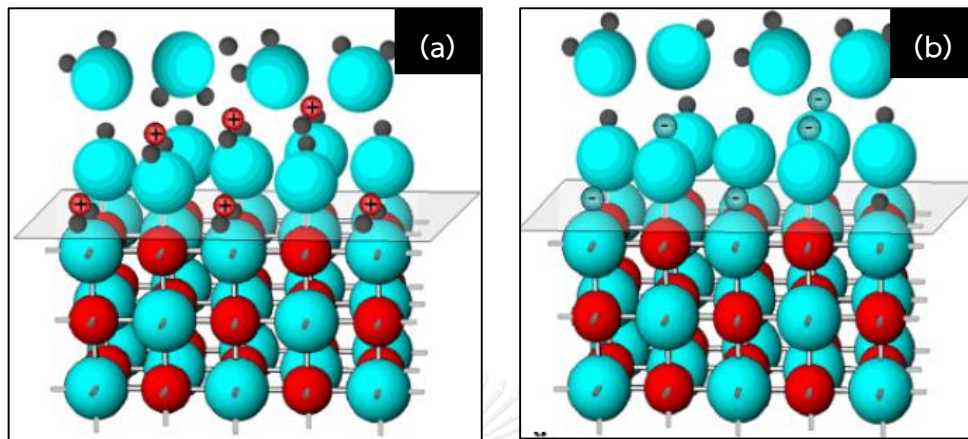


**Figure 4.47** The surface metal model for the atomic arrangements on (a) positively charged surface and (b) negatively charged surface [31].

When the external forces interfered the two surfaces in the system, the counterions had changed their concentration. According to the Figure 4.47, the blue spheres, the red spheres and the small gray spheres represented oxygen, the metal cations (in this research is  $Al_{3+}$ ), and hydrogen, respectively. If the surface is created with a positive charge (Fig. 4.46a), the  $Me-OH_2^+$  formation will be the major ion species. Likewise, if the surface is created with the negative charge (Fig. 4.47b), the  $Me-O^-$  species is fully formed in the system [31].

According to the equation and the atomic arrangements, it should be noted that the  $OH^-$  group is more reactive on the specimen, which connected to the positive electrode. This criterion is based on the law of attraction. Moreover, this specimen has a higher chance to form the defect more than the specimen that is connected to the negative electrode. From these results, it can be ensured that the

majority cause of the defect is the hydroxyl ions, which is consistent with the initial hypothesis.



## CHAPTER V

### CONCLUSION AND RECOMMENDATION

#### 5.1 Summary of the results

The results from this research can be concluded as following.

1. The corrosion behavior on the alumina coating depends on the temperature, the exposure time, and the operating environments.
2. The amount of dissolved oxygen in deionized water does not affect to the defect formation of the amorphous alumina in this system.
3. The high water pH has the higher chance for defect formation than the low water pH because the surface sites of the alumina are covered with the OH-group.
4. The addition of some ions in the solution may prevent the defect formation because these ions can form complex with water or react with the aluminium ions. These reactions resulted in the generation of the new protective layer that does not contain the OH group on alumina surface.
5. The corrosion behavior of this system is related to the electron transfer. The high voltage which applied in the solution resulted in the defect formation. This defect can be found at the negative electrode more than that found at the positive electrode. This result can be described by the electrolysis reaction.

6. When considered the effect of dissolved oxygen coupled with the electron transfer, the behavior of this system has a change. However, it does not have the appropriate reaction mechanism to describe.

7. The increasing of the electric potential resulted in the higher water dissociation which leads to the defect formation.

8. The amount of counterions (including hydroxyl ions) between the two electrodes surface has different concentration. This amount depends on the electric potential that applied in the system. The specimens which are located near the positive electrode have the chance for the defect formation higher than the specimens which are located near the negative electrode.

## 5.2 Conclusions

The corrosion in this work is the result from the hydrolysis reaction between the amorphous alumina and water. This reaction is represented for the defect formation on the surface. There are many factors that directly affect the defect formation and lead to the specimen corrosion. One of the most important factors causing the defect is originated from the hydroxyl group. There have many proposed methods to prevent this problem. Nevertheless, the application depends on the limitation of the process operating condition in each industry.

### 5.3 Recommendations

According to the mentioned conclusions, the recommendations for further studies in the industries are;

1. The conclusions are only based on the laboratory scale. For an application to scale up, the consideration of other factors is needed.
2. The intrinsic reaction between the amorphous alumina and water should be studied in more details.
3. The resistance of the alumina layer should be measured in order to supply the actual electric potential for driving the reaction.
4. In terms of the surfactant recommendation, this system should use the anionic surfactant because it may attach to the alumina surface better than the OH group since this reaction resulted in the OH replacement.

## REFERENCES

- [1] Edlmayr, V., Moser, M., Walter, C., and Mitterer, C. Thermal stability of sputtered Al<sub>2</sub>O<sub>3</sub> coatings. Surface and Coatings Technology 204(9–10) (2010): 1576-1581.
- [2] Ćurković, L. and Jelača, M.F. Dissolution of alumina ceramics in HCl aqueous solution. Ceramics International 35(5) (2009): 2041-2045.
- [3] Metson, J. 2 - Production of alumina. in Lumley, R. (ed.)Fundamentals of Aluminium Metallurgy, pp. 23-48: Woodhead Publishing, 2011.
- [4] Herrmann, M. and Klemm, H. 2.15 - Corrosion of Ceramic Materials. in Sarin, V.K. (ed.)Comprehensive Hard Materials, pp. 413-446. Oxford: Elsevier, 2014.
- [5] Zarras, P. and Stenger-Smith, J.D. 1 - Corrosion processes and strategies for prevention: an introduction. in Makhlof, A.S.H. (ed.)Handbook of Smart Coatings for Materials Protection, pp. 3-28: Woodhead Publishing, 2014.
- [6] Hihara, L.H. Chapter 1 - Electrochemical Aspects of Corrosion-Control Coatings. in Tiwari, A., Rawlins, J., and Hihara, L.H. (eds.),Intelligent Coatings for Corrosion Control, pp. 1-15. Boston: Butterworth-Heinemann, 2015.
- [7] Popov, B.N. Chapter 2 - Thermodynamics in the Electrochemical Reactions of Corrosion. in Popov, B.N. (ed.)Corrosion Engineering, pp. 29-92. Amsterdam: Elsevier, 2015.
- [8] Gurrappa, I. and Yashwanth, I.V.S. Chapter 2 - The Importance of Corrosion and the Necessity of Applying Intelligent Coatings for Its Control. in Tiwari, A., Rawlins, J., and Hihara, L.H. (eds.),Intelligent Coatings for Corrosion Control, pp. 17-58. Boston: Butterworth-Heinemann, 2015.
- [9] Ćurković, L., Jelača, M.F., and Kurajica, S. Corrosion behavior of alumina ceramics in aqueous HCl and H<sub>2</sub>SO<sub>4</sub> solutions. Corrosion Science 50(3) (2008): 872-878.
- [10] Gan, B.K., Madsen, I.C., and Hockridge, J.G. In situ X-ray diffraction of the transformation of gibbsite to  $\alpha$ -alumina through calcination: effect of particle size and heating rate. Journal of Applied Crystallography 42(4) (2009): 697-705.

- [11] Oda, K. and Yoshio, T. Hydrothermal Corrosion of Alumina Ceramics. Journal of the American Ceramic Society 80(12) (1997): 3233-3236.
- [12] Schacht, M., Boukis, N., and Dinjus, E. Corrosion of alumina ceramics in acidic aqueous solutions at high temperatures and pressures. Journal of Materials Science 35(24) (2000): 6251-6258.
- [13] Genthe, W. and Hausner, H. Influence of chemical composition on corrosion of alumina in acids and caustic solutions. Journal of the European Ceramic Society 9(6) (1992): 417-425.
- [14] Barinov, S.M., Ivanov, N.V., Orlov, S.V., and Shevchenko, V.J. Influence of environment on delayed failure of alumina ceramics. Journal of the European Ceramic Society 18(14) (1998): 2057-2063.
- [15] Sherif, E.S.M. Corrosion and corrosion inhibition of aluminum in arabian gulf seawater and sodium chloride solutions by 3-amino-5-mercapto-1,2,4-triazole. International Journal of Electrochemical Science 6(5) (2011): 1479-1492.
- [16] Gulicovski, J.J., Čerović, L.S., and Milonjić, S.K. Point of Zero Charge and Isoelectric Point of Alumina. Materials and Manufacturing Processes 23(6) (2008): 615-619.
- [17] Özer, N., Cronin, J.P., Yao, Y.-J., and Tomsia, A.P. Optical properties of sol-gel deposited Al<sub>2</sub>O<sub>3</sub> films. Solar Energy Materials and Solar Cells 59(4) (1999): 355-366.
- [18] Na, S., Jinhua, C., Cui, M., and Khim, J. Sonophotolytic diethyl phthalate (DEP) degradation with UVC or VUV irradiation. Ultrasonics Sonochemistry 19(5) (2012): 1094-1098.
- [19] Farooq, M. and Ramli, A. The determination of point zero charge (PZC) of Al<sub>2</sub>O<sub>3</sub>-MgO mixed oxides. in National Postgraduate Conference (NPC), 2011, pp. 1-5, 2011.
- [20] Li, J., et al. Corrosion analysis, and use of an inhibitor in oil wells. Research on Chemical Intermediates 40(2) (2014): 649-660.
- [21] Nunes, A.P.L., Peres, A.E.C., de Araujo, A.C., and Valadão, G.E.S. Electrokinetic properties of wavellite and its floatability with cationic and anionic collectors. Journal of Colloid and Interface Science 361(2) (2011): 632-638.

- [22] Del Nero, M., Galindo, C., Barillon, R., Halter, E., and Madé, B. Surface reactivity of  $\alpha$ -Al<sub>2</sub>O<sub>3</sub> and mechanisms of phosphate sorption: In situ ATR-FTIR spectroscopy and  $\zeta$  potential studies. Journal of Colloid and Interface Science 342(2) (2010): 437-444.
- [23] Ting-Ting, Z., Zhong-Xi, S., Xiao-Fang, Y., and Holmgren, A. Sorption of phosphate onto mesoporous  $\gamma$ -alumina studied with in-situ ATR-FTIR spectroscopy. Chemistry Central Journal 6(1) (2012): 26-35.
- [24] Miyazaki, A., Balint, I., and Nakano, Y. Solid-liquid interfacial reaction of Zn<sup>2+</sup> ions on the surface of amorphous aluminosilicates with various Al/Si ratios. Geochimica et Cosmochimica Acta 67(20) (2003): 3833-3844.
- [25] Lin, M.-Y., Hourng, L.-W., and Kuo, C.-W. The effect of magnetic force on hydrogen production efficiency in water electrolysis. International Journal of Hydrogen Energy 37(2) (2012): 1311-1320.
- [26] Philpott, M.R. and Glosli, J.N. Electric potential near a charged metal surface in contact with aqueous electrolyte. Journal of Electroanalytical Chemistry 409(1–2) (1996): 65-72.
- [27] Kelly, N.A. 6 - Hydrogen production by water electrolysis. in Basile, A. and Iulianelli, A. (eds.), Advances in Hydrogen Production, Storage and Distribution, pp. 159-185: Woodhead Publishing, 2014.
- [28] Millet, P. and Grigoriev, S. Chapter 2 - Water Electrolysis Technologies. in Diéguez, L.M.G.A.M. (ed.) Renewable Hydrogen Technologies, pp. 19-41. Amsterdam: Elsevier, 2013.
- [29] Senftle, F.E., Grant, J.R., and Senftle, F.P. Low-voltage DC/AC electrolysis of water using porous graphite electrodes. Electrochimica Acta 55(18) (2010): 5148-5153.
- [30] Ito, M. Structures of water at electrified interfaces: Microscopic understanding of electrode potential in electric double layers on electrode surfaces. Surface Science Reports 63(8) (2008): 329-389.

- [31] Franks, G.V. and Gan, Y. Charging Behavior at the Alumina–Water Interface and Implications for Ceramic Processing. Journal of the American Ceramic Society 90(11) (2007): 3373-3388.





APPENDICES

จุฬาลงกรณ์มหาวิทยาลัย  
CHULALONGKORN UNIVERSITY

## APPENDIX A

## CALCULATION THE CONCENTRATION OF ION IN AQUEOUS SOLUTION

**1. Preparation of anions in concentration at 20 ppb, 100 ppb and 500 ppb.**

The solution was prepared at 20 ppb of  $\text{Cl}^-$ ,  $\text{Br}^-$ ,  $\text{NO}_3^-$  and  $\text{PO}_4^{3-}$ , which each kind of anion has initial concentration of standard solution at 200 ppm. It has to make a new solution with lower concentration.

At aqueous solution at 20 ppb is refer to in one gram of water, it has the ion  $20 \times 10^{-9}$  gram. When letting final mass of water is equal to 500 grams, it should have amount of ion about  $500 \times 20 \times 10^{-9} = 1 \times 10^{-5}$  gram.

Standard solution has a concentration at 200 ppm means in one gram of water, it has ion  $2 \times 10^{-6}$  gram. If we need amount of ion is  $1 \times 10^{-5}$  gram, we will use the solution from standard  $(1 \times 10^{-5}) / (2 \times 10^{-6}) = 0.05$  gram.

Thus, at 20 ppb it has to use mass of solute from standard 0.05 gram dissolved in a total solution of water exactly 500 grams, while at the concentration up to 100 ppb and 500 ppb, the mass of standard solution were enhanced to 5 times and 25 times, respectively.

## 2. Preparation of cations in concentration at 20 ppb, 100 ppb and 500 ppb.

Cations were used in this experiment consists of  $\text{Mg}(\text{NO}_3)_2$ ,  $\text{ZnSO}_4$  and  $\text{Al}(\text{NO}_3)_3$ , which was in solid form. The properties of these reagents as followed.

Reagents: Magnesium nitrate ( $\text{Mg}(\text{NO}_3)_2 \cdot 6\text{H}_2\text{O}$ )  
Molecular weight = 148.31 g/mol  
(not included molecule of water)  
Standard atomic weight of Mg = 24.30 g/mol  
Assay of compound = 99.0%

Reagents: Zinc sulphate ( $\text{ZnSO}_4 \cdot 7\text{H}_2\text{O}$ )  
Molecular weight = 161.47 g/mol  
(not included molecule of water)  
Standard atomic weight of Zn = 65.38 g/mol  
Assay of compound = 99.0%

Reagents: Aluminium nitrate nonahydrate ( $\text{Al}(\text{NO}_3)_3 \cdot 9\text{H}_2\text{O}$ )  
Molecular weight = 212.99 g/mol  
(not included molecule of water)  
Standard atomic weight of Al = 26.98 g/mol  
Assay of compound = 98.0%

**Example:** For preparation of aqueous solution mixed with  $Zn^{2+}$  ion in concentration at 100 ppb.

Let target volume of mass is equal to 500 g.

The concentration at 100 ppb refer to in 1 g of water has  $Zn^{2+}$  ion  $100 \times 10^{-9}$  g.  
 If we need the final mass volume is 500 g,  $Zn^{2+}$  ion was used  $500 \times 100 \times 10^{-9} = 5 \times 10^{-5}$  g.  
 Thus, we have to use  $(5 \times 10^{-5} \times 161.47) / 65.38 \times 0.99 = 0.137$  mg of  $ZnSO_4$  and add water until 500 g to get the aqueous solution mixed with  $Zn^{2+}$  ion in concentration at 100 ppb.

Hence:

A = molecular weight of reagent

B = standard atomic weight of element

C = purity of component (assay)

In other words, at the concentration of 100 ppb, we have to use amount of  $ZnSO_4$  is  $(5 \times 10^{-5} \times A) / B \times C$  g. This formula is easy for adaptation in other concentrations.

At the concentration of  $Zn^{2+}$  ion with 20 ppb. =  $0.137 / 5 = 0.0274$  mg.

At the concentration of  $Zn^{2+}$  ion with 100 ppb. = 0.137 mg.

At the concentration of  $Zn^{2+}$  ion with 500 ppb. =  $0.137 \times 5 = 0.685$  mg.

**For preparation of aqueous solution mixed with  $Mg^{2+}$  ion in any concentrations.**

At the concentration of  $Zn^{2+}$  ion with 20 ppb. =  $0.308 / 5 = 0.0616$  mg.

At the concentration of  $Zn^{2+}$  ion with 100 ppb. = 0.308 mg.

At the concentration of  $Zn^{2+}$  ion with 500 ppb. =  $0.308 \times 5 = 1.54$  mg.

For preparation of aqueous solution mixed with  $\text{Al}^{3+}$  ion in any concentrations.

At the concentration of  $\text{Al}^{3+}$  ion with 20 ppb. =  $0.4027/5 = 0.0805$  mg.

At the concentration of  $\text{Al}^{3+}$  ion with 100 ppb. =  $0.4027$  mg.

At the concentration of  $\text{Al}^{3+}$  ion with 500 ppb. =  $0.4027 \times 5 = 2.0135$  mg.



## APPENDIX B

MEASURING AVERAGE PARTICLE SIZE AND HIGH OF OH<sup>-</sup> PEAK

## 1. Measuring average particle size of the specimen

The average particle size was measured after SEM analysis, which identified the corrosion in terms of formation of defect. This measuring performed by choosing the defect from SEM images less than 100 points/image and taking it into image processing program. We can get the average particle size as shown in the example below.

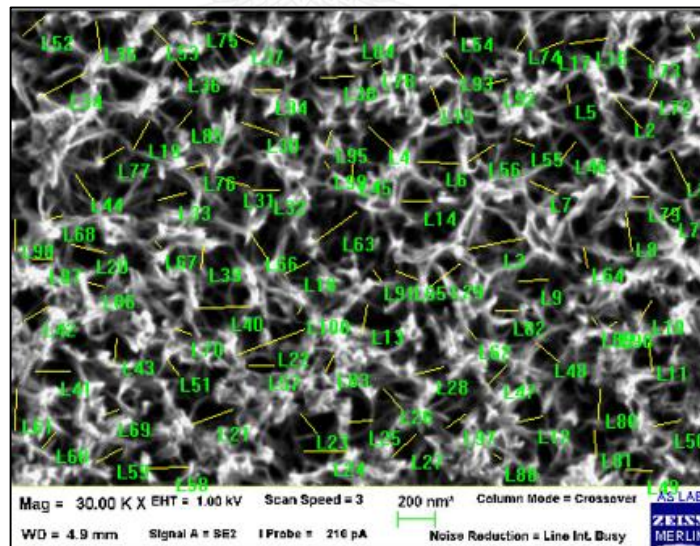


**Figure B.1** Example of measuring average particle size of the specimen after corrosion testing at 60 °C for 60 minutes.

## 2. Example of measuring high of OH<sup>-</sup> peak by ATR-FTIR analysis

After measuring the defect by ATR-FTIR analysis, we can get amount of OH<sup>-</sup> group in each condition as shown in Figure B.2.

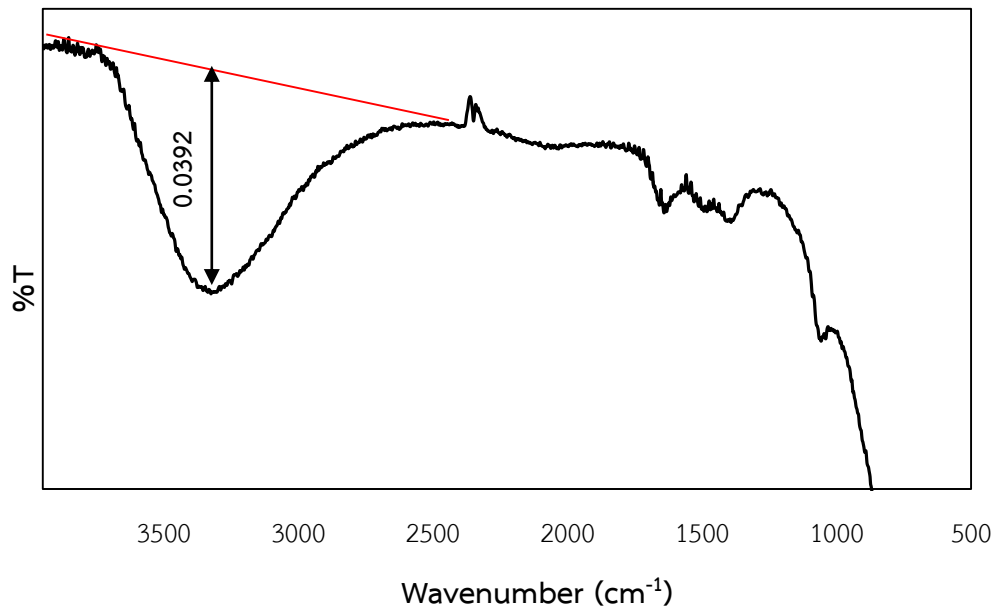


**Figure B.2** High of OH<sup>-</sup> peak after immersing the specimen into DI water at 50 °C for 120 minutes.

## APPENDIX C

## CALCULATION OF AQUEOUS SOLUTION WITH ANY PH VALUES

## 1. Preparation of aqueous solution with pH of 4 (acid solution).

Assumptions:      pH of DI water is 5.706  
                          We need aqueous solution with pH of 4  
                          Let final volume about 400 ml.

Formula:            pH      =  $-\log [H^+]$   
                          5.706 =  $-\log [H^+]$   
                           $[H^+] = 10^{-5.706}$   
                           $[H^+] = 1.967 \times 10^{-6} \text{ M.}$

If final volume is 400 ml.      =  $(1.967 \times 10^{-6} \times 400) / 1000$   
    =  $7.868 \times 10^{-7} \text{ mol. ....(1)}$

If we need to adjust pH of DI water is equal to 4

pH      =  $-\log [H^+]$   
 $[H^+] = 10^{-4}$

Final volume is 400 ml.      =  $(1 \times 10^{-4} \times 400) / 1000$   
    =  $4 \times 10^{-5} \text{ mol. ....(2)}$

(1) - (2)                              =  $3.92 \times 10^{-5} \text{ mol.}$

We have hydrochloric acid (HCl) with  $0.1 \text{ mol/dm}^{-3}$

Thus,                               $(3.92 \times 10^{-5} \text{ mol}) \times (1/0.1 \text{ dm}^{-3}/\text{mol})$   
    =  $3.921 \times 10^{-4} \text{ dm}^{-3}$  or 392.1  $\mu\text{L}$ .



So, at pH of 7, we have to use amount of NaOH with  $0.1 \text{ mol/dm}^{-3}$  about  $0.468 \text{ }\mu\text{L}$  in order to adjust aqueous solution which has final volume is 500 ml. Likewise, at pH of 9, we have to use 0.1M of NaOH about  $49.96 \text{ }\mu\text{L}$  as well.



## APPENDIX D

## LIST OF PUBLICATION

1. Vipada Dokmai and Varong Pavarajarn. "ALUMINA CORROSION IN DEIONIZED WATER". Proceedings of the Joint Conference on Renewable Energy and Nanotechnology 2014, Kanchanaburi, Thailand, December 22-23, 2014.



## VITA

Miss Vipada Dokmai was born on February 2, 1991 in Nakhon-ratchasima province, Thailand. In 2013, she received and got the second class honor in Bachelor's Degree of Chemical Engineering from Khon Kean University. Her senior project studied about the developing precise model of corrosion and fouling monitoring in condenser. She had an experience in operation engineering at Gulf Power Generation. After that, she gained admission to Graduated School of Chulalongkorn University in Center of Excellence in Particle Technology and graduated in 2015 with the thesis entitled "Alumina Corrosion in Deionized water".

